Comparative Analysis of the Morphological Characteristics of the Retractor Penis Magnus in Snake Copulation

by

Autumn S. Lee

A Paper Presented to the

Faculty of Mount Holyoke College in

Partial Fulfillment of the Requirements for

the Degree of Bachelors of Arts with

Honors

Department of Biological Sciences

South Hadley, MA 01075

May 2024

This paper was prepared

under the direction of

Prof. Patricia Brennan

for eight credits.

ACKNOWLEDGMENTS

My gratitude goes out to Dr. Patricia Brennan for being an amazing mentor and for teaching me the skills and knowledge I needed for this thesis. I am also grateful to Dr. Rachel Keeffe for being an inspiring PI in our lab, and for collecting the bulk of the RPM samples for this thesis. I would also like to thank my lab peers for the support and community they provided me throughout my time in the Brennan Lab (specifically: Catherine Paredes-Amaya, Ella Barton, Arin Rinvelt, Ray Larson, Grace Thompson, Maeesha Tasnim Naomi, Joanita Young, Aida Anaglo, and Jaimie Myong). In addition, I would like to thank Heather Hamilton for teaching me the necessary skills for utilizing the light microscope. Thanks also go out to my second and third committee members for reading my thesis and providing feedback (Dr. Gary Gillis and Dr. Wesley Yu respectively). Finally, I am very thankful to my family for supporting me throughout my college education here at Mount Holyoke. My life would not be what it is today if it weren't for all these incredible people and this inspiring community.

TABLE OF CONTENTS

List of Figures

List of Tables

Abstract

Until now, little was known about the morphological characteristics of the *retractor penis magnus* and its relationship with the hemipenis during copulation. Prior research describes only the basic function of pulling back in and retracting the everted hemipenis. However, more recent studies have observed morphological aspects of the retractor penis muscles suggesting a function beyond retraction. In addition, observations in the Brennan Lab of the muscle compared to the hemipenis have also suggested that size does not necessarily correlate between the two structures, raising further questions regarding the purpose and function of this structure during copulation. Through histological analysis, we gained a deeper understanding of the complex interplay between form and function of this structure, enabling us to draw more accurate conclusions about its function. In particular, there is evidence that this muscle provides rigidity to the hemipenis during copulation by its fiber arrangement. The findings from this study could offer broader implications for understanding sexual selection, reproductive strategies, and evolutionary patterns in snakes. Through this multidisciplinary approach, the study aims to enhance our understanding of the complex interplay between form and function in snake reproductive organs, offering valuable insights into the evolutionary biology of snakes and potentially other reptiles.

Keywords: Retractor penis magnus, histology, copulation, hemipenis

Introduction

The reproductive behavior and morphology of Squamates are unique across vertebrates. Squamates are the only order that has evolved to have unique paired intromittent organs known as hemipenes (King, 1981). However, whether paired hemipenes evolved due to selection or as a developmental byproduct remains unknown (Porto et. al, 2013). Intromittent organs are thought to have arisen with the evolution of the reptilian egg when internal fertilization became necessary during terrestrial life (Kelly, 2002). Furthermore, unlike the intromittent organs of most other amniotes such as mammals, archosaurs and turtles that have a single genital tubercle, lizards and snakes have paired genital tubercles that remain separate during development (Grelder, 2014). These paired genital turbecles are hemipenises, each one having a groove to carry sperm and a surface often covered with papillae, flounces, and/or spines (Dowling & Savage, 1960). Hemipenis morphology varies widely among snake taxa and includes cylindrical, bulbous, bilobed, and deeply divided structures ornamented with flounces, calyces, papillae, and spines (Dowling & Savage, 1960). Notably, these ornamental structures, specifically spines, are not common among lizards, whereas they are widespread throughout snake taxa (Olsson & Madsen, 1998). Higher order taxa are believed to have traded transverse flounces for spines which are usually largest near the base of the organ and decrease in size toward the apex

(Clark, 1945). Since Dowling and Clark, researchers have theorized that these spines may facilitate copulation either anchoring or playing a stimulatory role for the female (Pisani, 1976; Murphy & Barker, 1980; Olsson & Madsen, 1998).

During copulation only one hemipenis is everted laterally from the cloaca of the male into the female at a time, so eversion and intromission occur simultaneously. Prior to copulation these structures are inverted and encapsulated in the tail, but when the male is ready to engage with the female, these organs are everted into the female's cloacal opening (see Figure 1 below for illustration of inversion and eversion). Propulsion of the hemipenes into the female, is understood as a combined effort of contraction from the propulsor and retractor muscles (Dowling & Savage, 1960). Completion of this eversion is believed to be brought about by blood filling the sinuses in the surrounding erectile tissue (Porto, et al., 2013). Once copulation is complete, the retractor penis muscles bring the hemipenes back into the tail, but more recent observations suggest that these muscles may function as a transport for blood in the central sinus as reported in Porto et al (2013). Understanding more in depth the mechanisms of this full process requires a closer examination of both the external and internal reproductive structures.

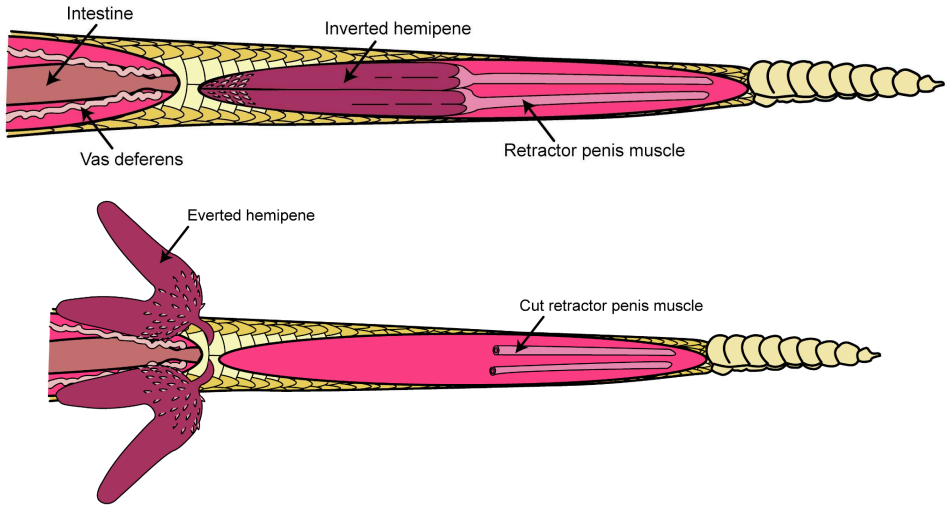

Above Illustration by: Dr. Rachel Keeffe

Figure 1: Illustration of dissected anterior ventral portion of a snake tail exposing the *retractor penis magnus* (RPM) and hemipene structure. The top depicts the hemipene inverted prior to copulation and bottom during copulatory acts with the RPM cut as a result of dissection.

Looking internally, we can examine the interior morphology of the hemipenis and its associated structures. The hemipenis consists of two concentric cylinders: the external *corpus cavernosum* and the internal *corpus cavernosum* (Dowling and Savage, 1960 & Porto et. al, 2013). The internal *corpus cavernos* is a hollow cylinder composed of loose connective tissue (Porto et. al, 2013). The external surface borders the inner muscular ring of the external *corpus cavernos*. Additionally, the hemipenis is lined with epithelial tissue, featuring smooth non-cornified layers in the trunk region and papillate cells in the capitulum (see Figure 2). Within the connective tissue, numerous irregular lacunar spaces exist,

which fill with blood during tumescence. The largest retractor penis muscle, the *retractor penis magnus,* traverses the internal corpus cavernos along its entire length, forming the inner wall of the *corpus cavernos* (Porto et. al, 2013). The muscle bifurcates as it reaches the hemipenis bifurcation. Externally, two veins travel together near the spermatic groove, originating from the internal *corpus cavernos* at the hemipenis base (Porto et. al, 2013). These veins course cranially and then separate into a venous bed situated dorsally and laterally to the cranial region of the hemipenis. The venous bed connects to the caudal vein running alongside the artery canal. These veins play a crucial role in draining blood from the hemipenis during detumescence (Porto et al., 2013).

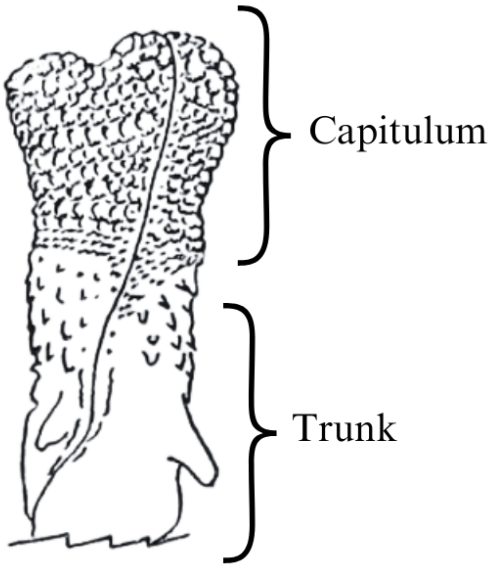

Figure 2: External anatomical features of the hemipenis taken from Dowling drawing.

Research on snake reproductive organs has long intrigued researchers due to the unique anatomical features and their significance in understanding sexual selection, reproductive strategies, and evolutionary patterns. Some of the earliest comprehensive scientific reports of the hemipenes and cloaca in lizards and snakes were from a German scientist Dr. Unterhossel (Reese, 1947). Noticing the variety and uniqueness of these structures intrigued scientists and spurred further investigation of the hemipenis. Despite the increasing interest in studying the function and structure of the hemipenis, the associated musculature responsible for retractor movements during copulation has been largely overlooked.

The retractor penis muscles in snakes were first described in 1650 by a British scientist named Edward Tyson, who named and illustrated the “rectractores penum" as a collection of muscles branching from the tail vertebrae to the end of an individual inverted hemipene. Actual research on the function of this structure was not until much later in 1960. In a volume of Zoologica titled: “A Guide to the Snake Hemipenis: a Survey of Basic Structure and Systematic Characteristics,” Dowling and Savage first describe the function of the muscle as to retract and pull in the everted hemipenis after copulation (see Figure 3).

Three groups of retractor muscles have been described in snakes (Serpentes): *retractor penis magnus, retractor penis parvus,* and *retractor penis basalis* (Dowling & Savage, 1960; Keogh, 1996). The *m. retractor penis magnus*,

the largest of the hemipenis retractor muscles, originates on one of the posterior caudal vertebrae and extends anteriorly to attach at the distal tip of the hemipenis (Dowling & Savage, 1960; Porto et al., 2013). The *m. retractor penis parvus* stems from one or more of the cranial caudal vertebrae (which is medial to the propulsors) and inserts by a flattened tendon on the dorsal auscultate surface of the hemipenis (Dowling & Savage, 1960; Porto et al., 2013). The *m. retractor penis basalis* originates from the ventral abdominal wall below the urogenital papilla and inserts via a strong and short tendon on the asulcate surface of the hemipenis (Dowling & Savage, 1960; Porto et al., 2013). Together these muscles relax and retract the hemipenis following copulation. However, as observed in rattlesnakes in the Porto et al paper, the first step of mechanical eversion is due to the action of the skeletal muscle *m. retractor penis basalis* (2013). When the snake raises its cloacal shield (opening the cloaca) for copulation, about one-fourth of the hemipenis is outfolded by the *m. retractor penis basalis.* Further dissection of this muscle revealed its propulsor action which is antagonistic to the other retractor penis muscles. The other muscles, the *m. retractor penis magnus* and *m. retractor penis parvus,* were conversely understood to function during inversion to pull back the everted hemipenis (Porto et al., 2013). However, as also observed in the Porto et al. paper, the *retractor penis magnus* has a bloodstream that runs into the muscle during tumescence suggesting it plays a role in eversion

as well (2013) For this study we examined the *retractor penis magnus,* which will henceforth be referred to simply by RPM, and all three of these muscles as RPMs.

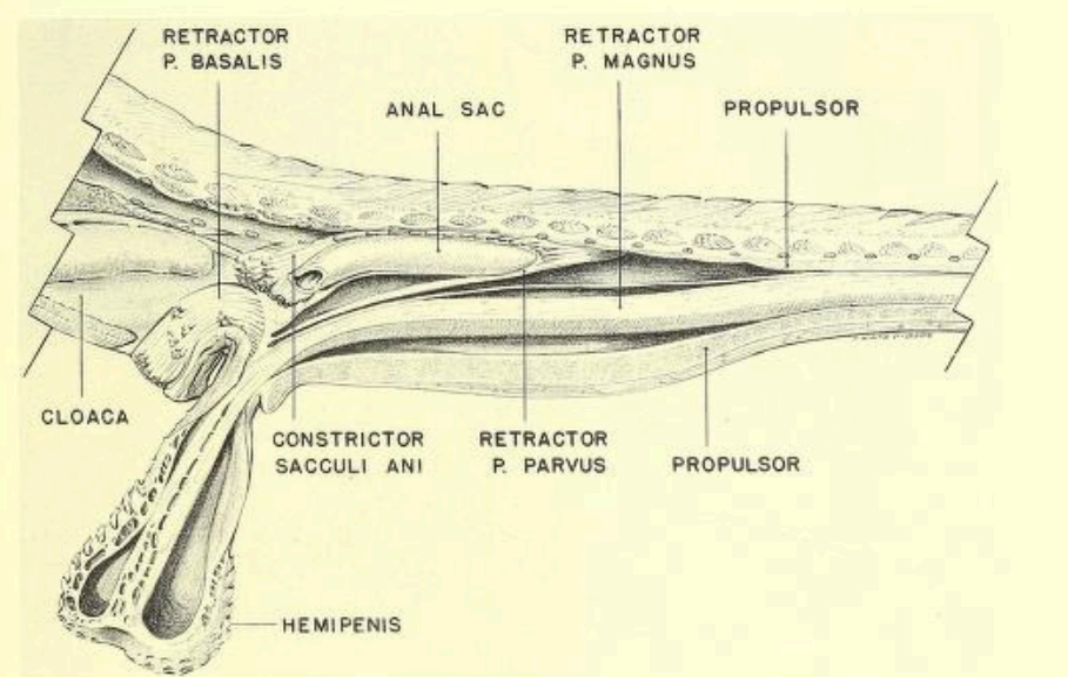

Credit: Dowling and Savage, 1960

Figure 3: Illustration of hemipenis structure and associated retractor penis muscles.

Muscles and/or ligaments responsible for penile retraction are not only found in squamates but are also found in mammals and other vertebrates. In mammals there are retractor penis muscles (RPMs) in many (but not all) species, in crocodilians there is a ligament that retracts the penis, and in birds there is also a ligament responsible for a similar copulatory behavior (Bassett, 1961 and Kelly, 2013). Notably, the RPMs found in Squamata have no homology to the RPMs

present in mammals, although both are understood as responsible for the retraction of the copulatory organ (Bassett, 2016). Furthermore, much like the state of existing literature on lizards and snake copulatory structures, very little is known about the copulatory structures in other vertebrates. Part of the limitations to our understanding is that copulation occurs internally, and as a result we cannot observe how these copulatory structures and corresponding muscles interact *in vivo*. However, we can address copulatory behavior of these organisms through other methods, such as modeling and rendering these structures in 3D. To better address the morphological evolution of genital morphology and the mechanisms that drive genital diversification, the Brennan Lab has focused on developing a comprehensive comparison of genitalia across all families in the suborder Serpentes (snakes).

Researchers have been able to investigate the hemipenis and the RPM more closely with technological advancements such as improved microscopes, histology, and chemical analyses (such as those described by Jensen, Grady W., et al. 2022), but their understanding of this particular muscle is limited, providing mainly functional descriptions and only limited insight into its morphology (specifically that the RPMs function for retraction of the hemipene). However, the full function of the RPMs during copulation still remains unclear. In a detailed morphological study of rattlesnake hemipenes, Porto et al (2013), illustrated that

there are lacunae and extensive vascularization throughout the RPMs that suggests that this muscle may play a role in hemipene eversion, not just retraction. They even went as far as to suggest a name change for one of these muscles, the *retractor penis basalis* to the musculus hemipenis propulsor given their findings. This opens the possibility that the larger muscle (*retractor penis magnus)* may also play a role in copulation beyond combined retraction. However, this proposed function is novel, with all prior sources mentioning only the combined role of the RPMs in reverting the hemipene into the tail after copulation is finished. Beyond function, the morphology of this muscle (RPM) is unique, primarily composed of skeletal muscle tissue and centrally traversed throughout its length by a narrow sinusoid consisting of a thin layer of smooth muscle lined by endothelium (as discussed in Porto, Marcovan, et al 2013). Prior observations in the Brennan Lab suggested that the size of the muscle does not necessarily correlate with the hemipenis size, raising questions about their interplay during copulation. These knowledge gaps highlight the need for a comprehensive comparative analysis of the morphological characteristics of the largest retractor penis muscle (*retractor penis magnus)* in squamates.

If this muscle functions in retraction then we would expect the morphology to reflect that function. Because skeletal muscle produces force in proportion to its overall diameter, a smaller diameter of individual fibers, coupled

with a specific arrangement, could enhance the perpendicular muscles' ability to amplify speed and displacement through contraction (Figure 4, Kier and Smith, 1985). Similarly, an RPM with a larger diameter (more fibers) could exert greater force during reversion of the hemipene back into the tail. By examining the morphological structure of the RPM, specifically the percentage of area fibers occupied in the transverse plane, as well as the diameter of the individual fibers, we hope to better understand the force these muscles would theoretically exert on the hemipenis. Additionally, we want to examine the diameter of these fibers in the transverse plane to better understand the hydrostatic relationship and address the question of whether the length of *retractor penis magnus* illustrate a relationship between hemipenis size (measured by volume) and RPM length.

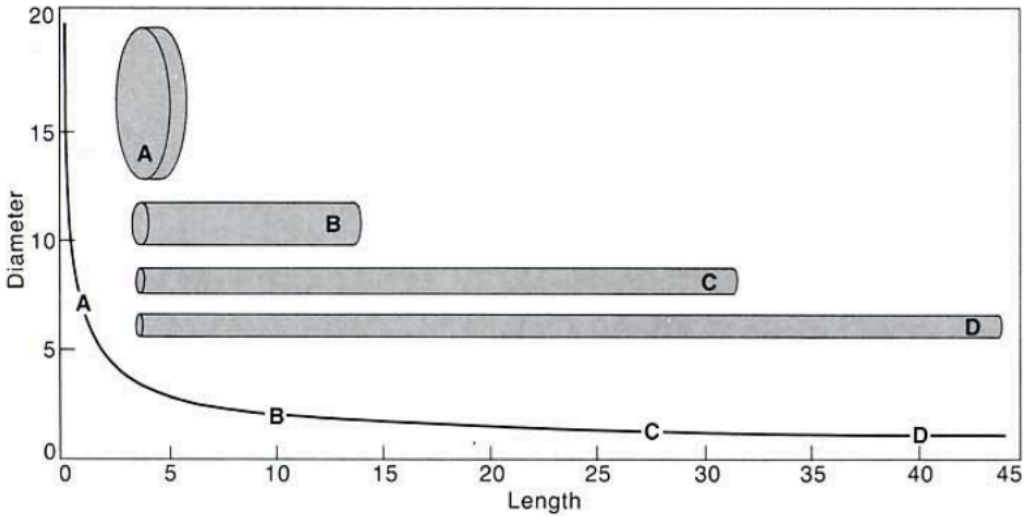

Credit: Smith and Kier 1989

Figure 4: The following diagram illustrates how perpendicular muscles can greatly enhance speed and displacement through contraction. When the length-to-diameter ratio is high, even a slight reduction in diameter results in a significant increase in length.

Through histological analysis and comparisons between different snake families, this study aims to uncover the morphological details of the *retractor penis magnus* and its relationship to the hemipenis. Specifically we expect that the RPM functions in eversion of the hemipene (similar to the findings of Porto et al., 2013) we also expect to find a relationship between the RPM's size (length and diameter) and the size of the hemipene (volume). If the RPM's size is a byproduct of the size of the tail of the snake, we would hypothesize that the snout ventral length (SVL, in other words body size) and tail length are more associated with the RPM size than the hemipene size. Furthermore, if the RPM functions in eversion of the hemipene, we would expect that larger hemipenes would require a muscle that can exert more force or that can expand more to allow blood to pass through. In this case we would expect larger RPM diameter given RPM length, larger fiber diameter, and/or higher density of fibers when hemipenes are larger. In addition, a pennate fiber arrangement (non-parallel fibers), would indicate an increase in force production as well by increasing the density of fibers in a given cross-sectional area. In order to address these questions effectively, a multidisciplinary approach was employed.

I utilized multiple methods to examine this muscle including macro-dissection, histology, quantification of tissues and statistical analyses of previously collected data to compare and analyze the morphological characteristics of the retractor penis muscle across different snake families. The goals of this study are as follows: 1) within species comparison of the size of RPM and the volume of inflated hemipenes, using data collected by the Brennan lab 2) between species comparison in multiple snake families to see if any phylogenetic patterns are evident, 3) histological examination of the RPM muscle in several snake species to determine fiber type, arrangement, variation in fiber size, density, and presence of vascularization that could be consistent with Porto's observations. The insights gained from this research not only contribute to our understanding of snake reproductive organs but also have broader implications for evolutionary biology and reproductive strategies in reptiles.

By addressing the current gaps in knowledge and drawing from previous research, this study endeavors to enhance our understanding of the complex interplay between form and function in snake reproductive organs. Ultimately, it aims to provide valuable insights into the evolutionary biology of snakes and potentially other reptiles.

Materials and Methods

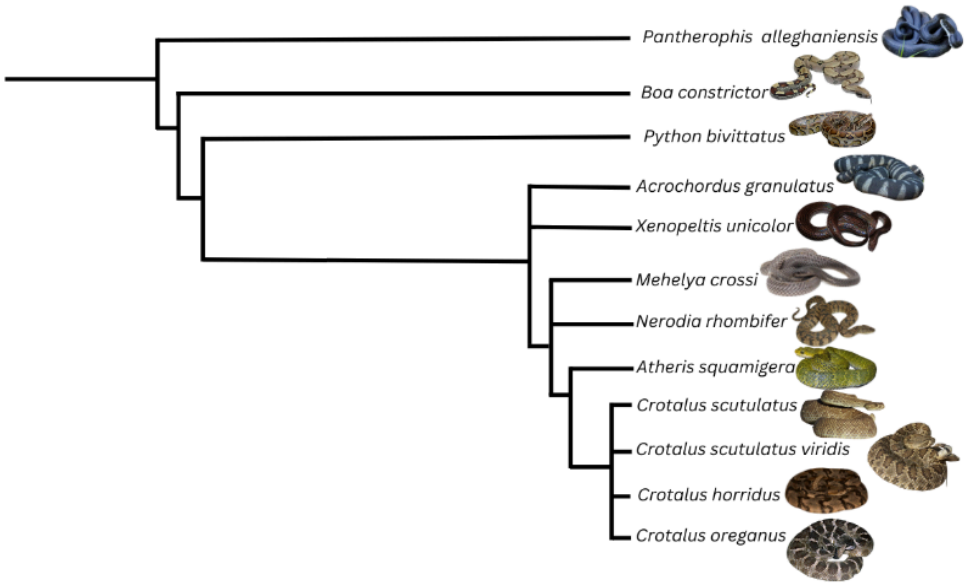

Figure 5: Phylogeny of 12 snake species utilized in this study, data taken from NCBI Taxonomy database.

Data Collection

For a comparative analysis between species, I extracted data and RPM samples from the following species for which we have an ample sample size: Colubridae *Nerodia rhombifer,* Viperidae *Crotalus scutulatus,* Viperidae *Crotalus scutulatus viridis,* Viperidae *Crotalus oreganus,* Acrochordidae *Acrochordus granulatus,* Viperidae *Atheris squamigera,* Colubridae *Pantherophis*

alleghaniensis, Xenopeltidae *Xenopeltis unicolor,* Viperidae *Crotalus horridus,* Lamprophiidae *Mehelya crossi,* Boidae *Boa constrictor* and Pythonidae *Python bivittatus* (phylogeny provided above, Figure 5). From this list I narrowed the species analysis of hemipene volume, SVL, and tail length to RPM length to the ones we had the most intact RPM specimens for comparison, and simplified the list to three families: Pythonidae *Python bivittatus,* Colubridae *Nerodia rhombifer,* and Viperidae *Crotalus scutulatus.*

Based on snake dissections that had been performed in the Brennan lab, I was able to use previously collected data on RPM length, tail length, and SVL. This allowed me to examine the relationship between RPM size and other parameters that might have influenced this muscle's unique morphology. As part of an ongoing genitalia study in the Brennan Lab, hemipene size was taken from previous dissections and 3D images were rendered through EinScan. I then imported these mesh scans into auto desk photo recapture, where I calculated the volume of the hemipenes utilizing auto desk's built-in measurement tools. The length of the retractor penis muscles was also measured prior to dissection, as part of the process to extract hemipenes involves cutting the RPM. For the comparative phylogenetic study of RPM, I included all the species for which we have RPM length data and hemipene volume, Colubridae *Nerodia rhombifer,* Viperidae *Crotalus scutulatus,* Viperidae *Crotalus scutulatus viridis,* Viperidae

Crotalus oreganus, Acrochordidae *Acrochordus granulatus,* Viperidae *Atheris squamigera,* Colubridae *Pantherophis alleghaniensis,* Xenopeltidae *Xenopeltis unicolor,* Viperidae *Crotalus horridus,* Lamprophiidae *Mehelya crossi,* Boidae *Boa constrictor* and Pythonidae *Python bivittatus*.

To collect this data I used the following protocol:

Histology

I utilized tissue sections from previously collected retractor penis muscles (RPM) from the above mentioned species that were preserved in 10% buffered formalin. These are the species for which we have collected the most RPM samples from, and have not been compared nor has this structure been examined in prior literature in these species.

The histology practice employed in this study follows standard paraffin histology protocols (see histology Tables 1-3 in the appendix). Tissue samples were sliced and immediately fixed in 10% neutral buffered formalin overnight. Following fixation, the samples were dehydrated using a graded series of ethanol solutions, embedded in paraffin wax, and sectioned into thin slices (4-6 μm) using a microtome. Because many of the samples were small in diameter, they were embedded with a needle to keep the transverse and sagittal orientation of the mount. The slice sections were then mounted onto glass slides and stained with hematoxylin and eosin (H&E) staining and Masson's trichrome, to visualize

cellular structures and tissue morphology. Finally, the slides were examined under a light microscope and representative images were captured for further analysis and documentation. ImageJ was then used to quantify fiber size and density from the histology photos.

For one specimen, we decided to try and fix the muscle open as it would be *in vivo* if blood fills in the central sinus of the RPM (see Figure 7 Part B). To do this we utilized a fresh sample from a *Crotalus scutulatus* specimen. We separated the muscle from the point of insertion on the hemipenis and inserted a wooden dowel into the muscle to keep it open. We also did this with vaseline to try a different method as well. Following this procedure I fixed and went through the steps of histology as outlined above.

Image J

Image J was utilized for analysis of light microscopy photos taken at 10x magnification. To measure the density of RPM fibers as well as fiber count, average size, and diameter, I first converted all transverse and sagittal photos into RGB stacks. Each photo yielded three corresponding black-and-white images (Fig. 2). We fine-tuned the threshold to remove most connective tissues while preserving muscle fibers. Subsequently, we specified a range to disregard area measurements from particles smaller than 25 μm^2. ImageJ then automatically measured the areas of the muscle fibers (Fig. 2). To calculate the densities, we

used the percentage area of white (fibers) provided in the automatic particle counting output.

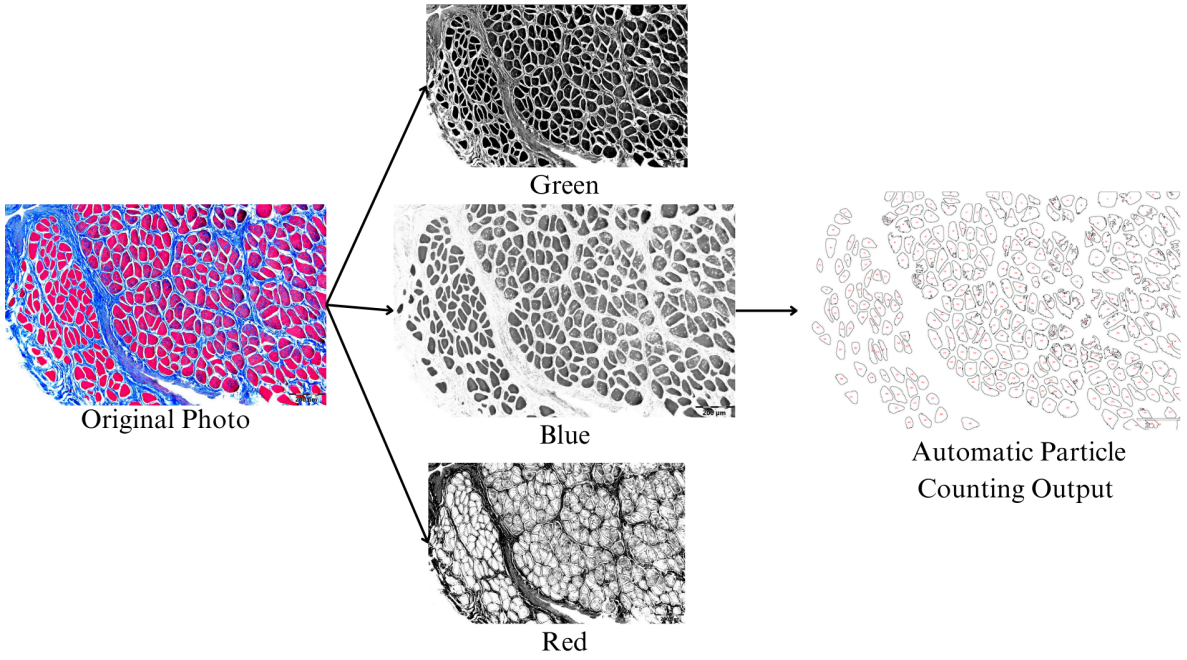

Figure 6: Workflow of collecting fiber measurements through ImageJ.

Statistical analysis

The statistical analysis in this study involved the use of R Studio and ImageJ software to compare hemipene size to the length of the *retractor penis magnus*. The data obtained from both direct measurements via dissection as well as hemipene volume data collected via Autodesk Photo Recapture were imported into R Studio for statistical analysis. Specifically I utilized a generalized linear

model to determine whether RPM size is predicted by hemipene volume, snout ventral length (SVL) or tail length (see RCode in appendix).

Results

RPM Length Size Comparisons

The first goal of this study was to gain an understanding of the general relationship between RPM length compared to hemipene volume, SVL and tail length. In order to understand if the RPM length was predicted by hemipene volume or by tail length, I conducted a one-way analysis of variance (ANOVA). The volume of the hemipenes is significantly associated with RPM length in all three species, $F(1, 46) = 1218.281$, $MSE = 66614$, $p < 2.2e\text{-}16$ (Figure 7).

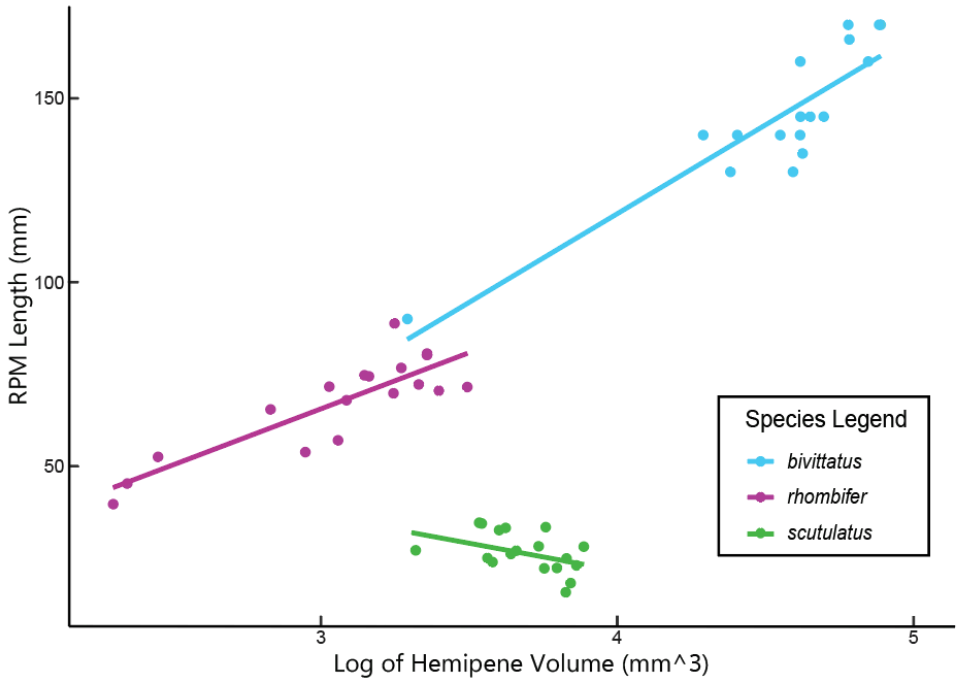

Figure 7: Generalized linear model depicting RPM length in mm on the y axis and the natural log of the hemipene volume on the x axis across three species: Pythonidae *Python bivittatus* (red), Colubridae *Nerodia rhombifer* (green), and Viperidae *Crotalus scutulatus* (blue).

Similarly, a one-way analysis of variance (ANOVA) was conducted to evaluate whether RPM length was significantly impacted by tail length. Tail length did have a statistically significant relationship to RPM length but, there was no statistically significant difference between tail length at the species level in either Bivittatus or Scuutlatus (Tail Length to RPM (species combined) $F(1, 31) = 381.85$, $MSE = 118523$, $p < 2.2e\text{-}16$; In Scutulatus $F(1, 15) = 0.6021$, MSE

= 17.066, p < 0.4498; In Bivittatus (1, 14) = 0.6168, MSE = 132.66, p < 0.4453).

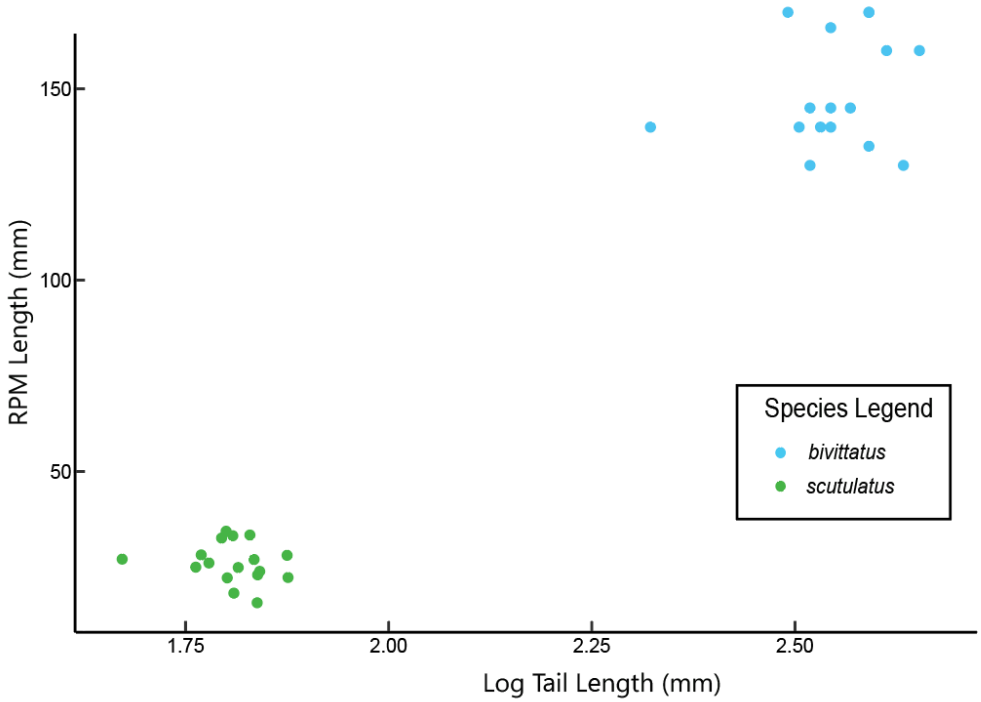

Figure 8: Generalized linear model depicting RPM length in mm on the y axis and the tail length in mm on the x axis across three species: Pythonidae *Python bivittatus* (red), Colubridae *Nerodia rhombifer*(green), and Viperidae *Crotalus scutulatus* (blue).

Finally, a one-way analysis of variance (ANOVA) was conducted to evaluate whether RPM length was significantly impacted by SVL. A statistically significant association was found between SVL and the RPM length, F(1, 50) = 156.28, MSE = 102318, p < 2.2e-16. (Figure 9).

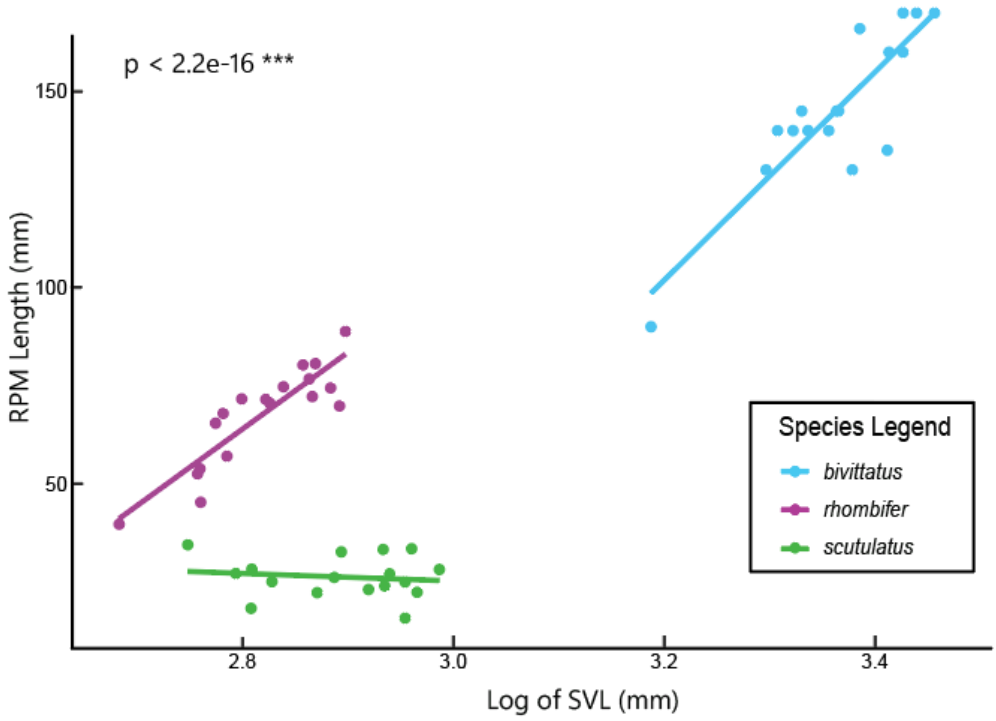

Figure 9: Generalized linear model depicting RPM length in mm on the y axis and the log of the SVL in mm on the x axis across three species: Pythonidae *Python bivittatus* (red), Colubridae *Nerodia rhombifer* (green), and Viperidae *Crotalus scutulatus* (blue).

We also ran a linear model to determine the relationship of the two independent variables we had for all three species (SVL and Hemipene Volume) compared to RPM length. The ANOVA results showed that both variables were individually significantly associated with RPM length (Hemipene Volume $F(1,48) = 162.33$, $MSE = 66614$, $p < 2.2e\text{-}16$; SVL $F(1,48) = 41803$, $MSE = 41803$, $p = 1.87\ e\text{-}13$), and also their combined effect was significantly associated with RPM length ($F(1, 48) = 16.91$, $MSE = 6939$, $p = 0.0001526$).

General Dissection Observations

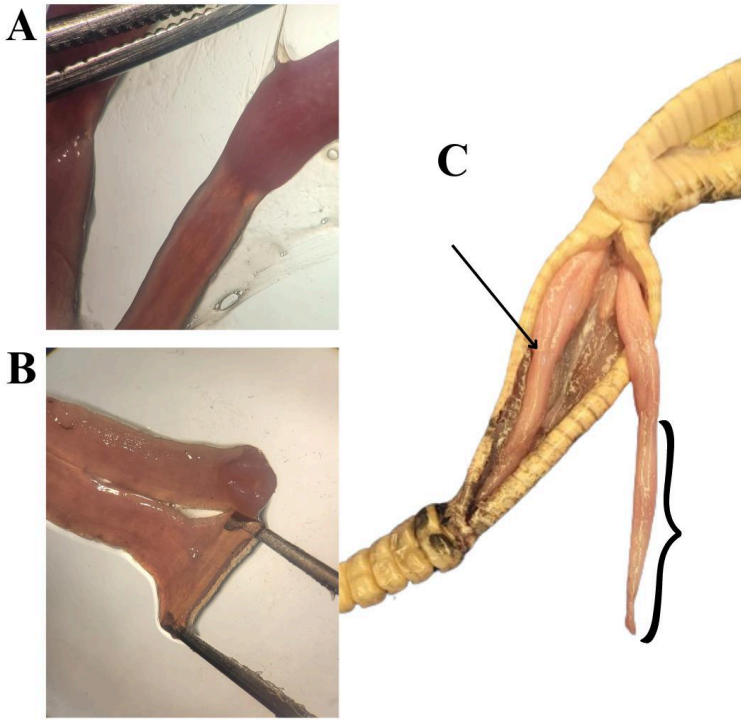

Figure 10: Closer examination of RPM in *Crotalus scutulatus.* A. RPM under a dissecting microscope highlighting the separation in color between RPM and Hemipene. The RPM is the lighter portion respectively and is beneath the darker portion which is above and is the hemipene. B. Stretching the muscle under a dissecting scope after detaching from hemipene, and highlighting the hollowness of the structure. C. RPM's in snake still attached to the hemipene, arrow pointing out the point where hemipene and RPM meet, and the bracket denoting the RPM length.

As previously mentioned, the *retractor penis magnus* (RPM) stands out as the largest among the three retractor muscles. Encased in approximately 5 to 8

layers of connective tissue, this muscle is notably hollow and exhibits remarkable flexibility, capable of increasing in length through manipulation. Upon closer examination using a dissecting microscope, the presence of skeletal muscle layers surrounding a sinusoidal space was confirmed (see figure 10 above). The opening to the sinus can be easily seen with the naked eye. The RPM is composed of two muscle bundles that run alongside each other, and either attach in the middle of the internal surface of the capitulum, or branch into two to attach to each lobe of the hemipenes when they are bilobed.

Histology Forcing the Sinusoid Open

In order to better visualize the extent to which fibers stretch around the open sinusoid, we fixed a specimen open. Through experimental trial and error, we used a wooden dowel to keep the sinusoid open during the dehydration and clearing phase of histology (see Figure 11). In this open transverse state the division of two concentric layers in the muscle is evident. The internal ring seems to have more densely packed fibers than the external ring.

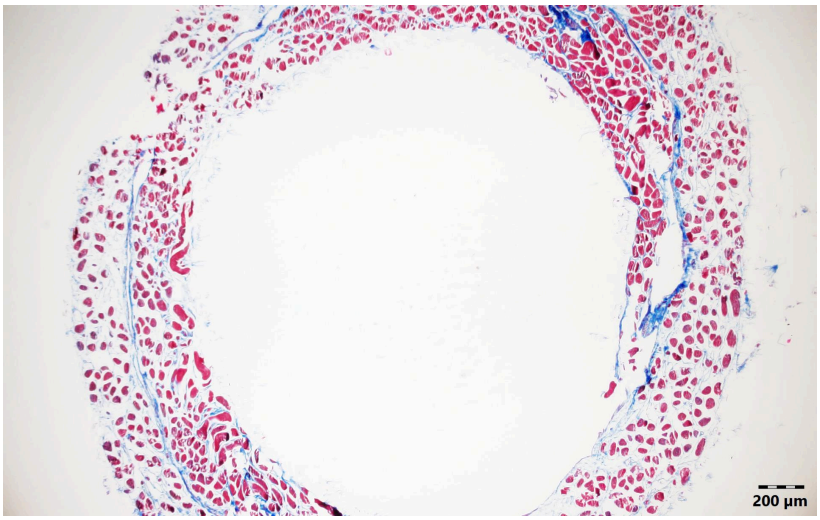

Figure 11: Mason's trichrome stain of a fixed open sinusoid from *Crotalus scutulatus.*

General Histological Observations

Research by Porto et al. (2013) categorizes the retractor penis muscle as skeletal muscle, and in this study we confirmed the presence of striated fibers in all species examined. Notably, the sinusoidal space was consistently visible in the transverse section across all species we examined as described in Crotalis (Porto et al., 2013).

Histological staining in both the transverse and sagittal planes revealed a complex arrangement of fibers (refer to Figure 32 in Appendix for understanding skeletal muscle). There appears to be some organization to the fibers, however the presence of fibers running both transverse and longitudinal in transverse sections is interesting because of how thin this muscle is and considering it is thought to be

only functioning for the main purpose of pulling back the everted hemipenis. All species observed had collapsed sinusoid spaces in some capacity and surrounding these collapsed spaces were pockets of fibers surrounded by connective tissue (see figures of individual species below).

Histological Observations by Species

Colubridae Nerodia rhombifer

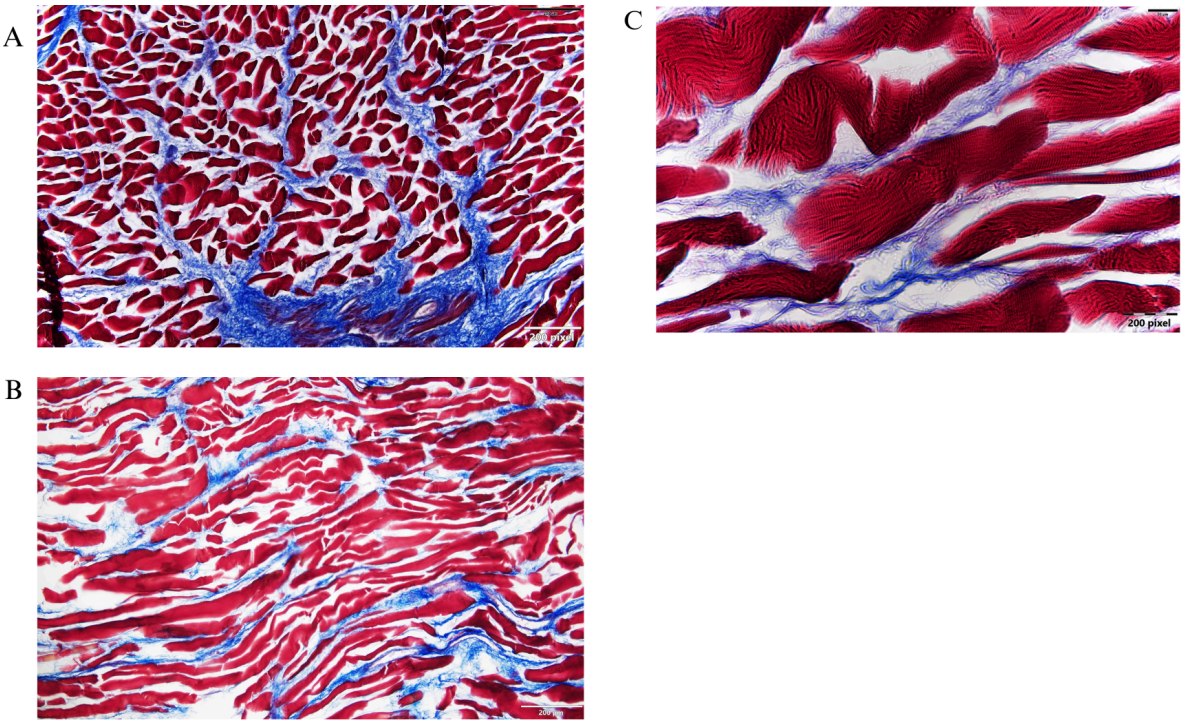

Figure 12: Mason's trichrome of *Nerodia Rhombifer.* A) Transverse section of RPM at 10x magnification. B) Sagittal section at 10x magnification. C) Muscle fibers at 50x magnification highlighting striated fibers indicative of skeletal muscle

The fiber arrangement in *Nerodia rhombifer* can provide several insights. Fibers are seen to run both longitudinally and pinnately in a cross section (Figure 12 panel A). Notice how the fibers are not circular and many are oval or long indicating the change in directionality. Furthermore, the arrangement seems random in Nerodia with the direction of muscle fibers running in many directions across the fascicle and around the collapsed sinus (bottom blue section of panel A). In the longitudinal section (Figure 12, panel B) fibers run in the same general parallel direction and seem to have a wavy quality to them. Finally, skeletal fiber is confirmed by the parallel striation seen in panel C of Figure 12.

Viperidae Crotalus scutulatus

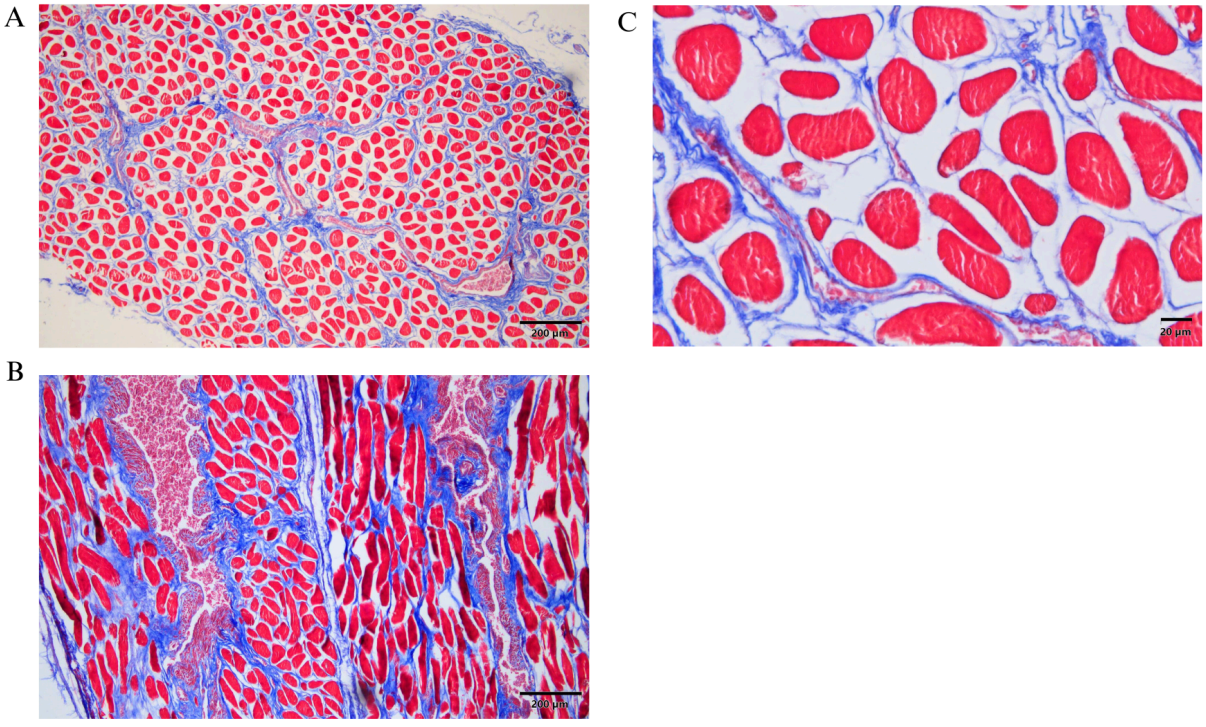

Figure 13: Mason's trichrome of *Viperidae Crotalus scutulatus* A) Transverse section at 10x magnification. B) Sagittal section at 10x magnification. C) Muscle fibers at 50x magnification highlighting striated fibers indicative of skeletal muscle

Crotalus scutulatus's fiber arrangement can provide a number of insights. Fibers are seen to run both longitudinal and pinnate in a cross section (Figure 13 panel A). Most fibers are fairly circular, however several fibers, especially on the periphery of the perimysium, are more oblong suggesting these fibers are running pinnately. Furthermore, the arrangement seems to have some sort of order in Crotalus with the direction of muscle fibers running largely longitudinal and many are a similar size (as seen in panel A). In the longitudinal section (Figure 13, panel B) fibers run both pinnately and longitudinally which is an unusual arrangement in this particular cross section. Finally, we observed fiber breakage indicating inflammation from recent use of this muscle (Figure 13, panel C).

Viperidae Crotalus scutulatus viridis

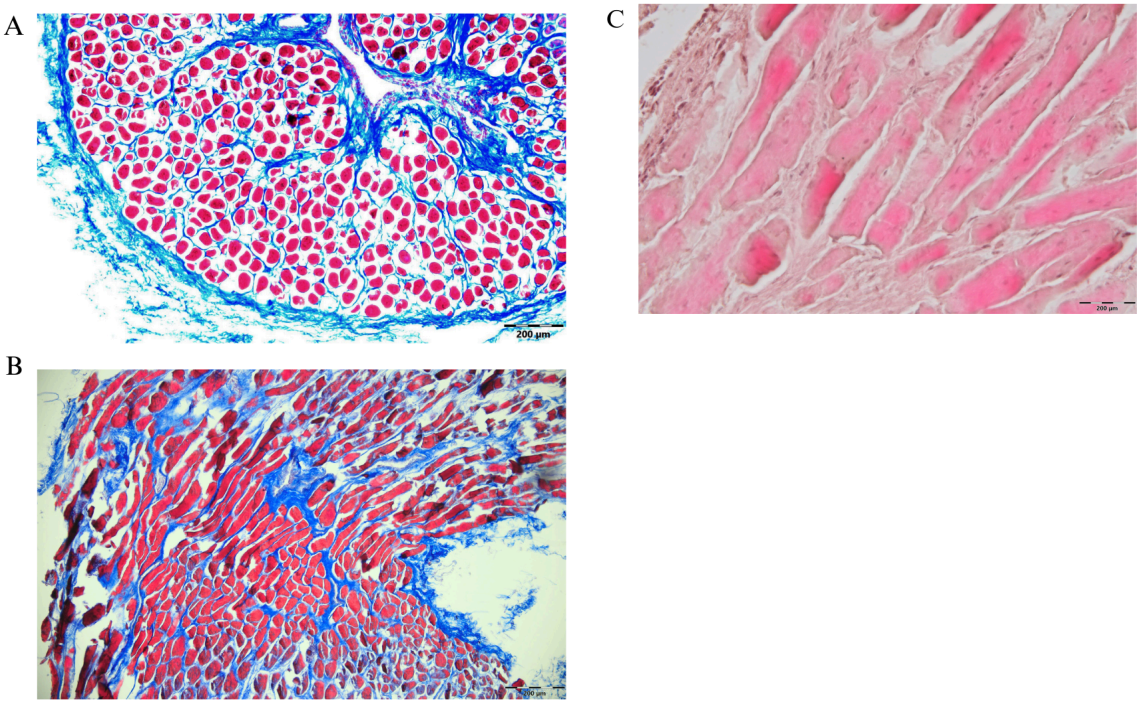

Figure 14: Mason's trichrome of *Viperidae Crotalus scutulatus viridis* A) Transverse section at 10x magnification. B) Sagittal section at 10x magnification. C) Muscle fibers at 50x magnification highlighting striated fibers indicative of skeletal muscle

The fiber arrangement of *Crotalus scutulatus viridis* can reveal a number of interesting aspects. Fibers are seen to run both longitudinally and pinnately in a cross section (Figure 14 panel A). Similar to *Crotalus scutulatus,* most fibers are fairly circular in the *viridis* hybrid. In this particular specimen, the sinusoid is not completely collapsed, and the perimysium seems thicker surrounding this region. Furthermore, the arrangement seems to have some sort of order in Crotalus with the direction of muscle fibers running largely longitudinal and many are a similar size (as seen in panel A). Additionally, like *Crotalus scutulatus* in the longitudinal section (Figure 14, panel B) fibers run both pinnately and longitudinal. Finally, we observed the random arrangement of a multitude of nuclei in panel C in an H&E stain (nuclei are purple dots).

Viperidae Crotalus oreganus

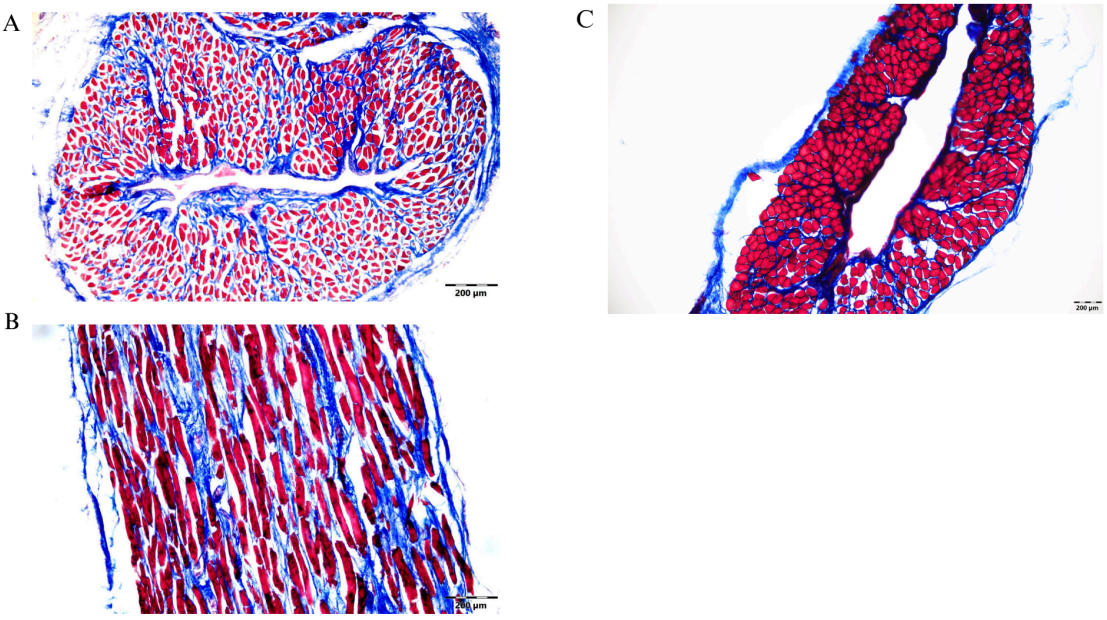

Figure 15: Mason's trichrome of *Viperidae Crotalus oreganus* A) Transverse section at 10x magnification. B) Sagittal section at 10x magnification. C) Muscle fibers at 50x magnification highlighting striated fibers indicative of skeletal muscle

In *Crotalus oreganus*, the fiber arrangement can reveal a range of interesting characteristics. Fibers are seen to run both longitudinally and pinnately in a cross section (Figure 15 panel A). Similar to Crotalus, most fibers are fairly circular, but size of fibers varied in the space they occupy in the endomysium. In this particular specimen, the sinusoid was not completely collapsed, and the perimysium seems thicker surrounding this region. Furthermore, the arrangement seemed to have some sort of order with the direction of muscle fibers running largely longitudinally (as seen in panel A). In the longitudinal section (Figure 15, panel B) fibers run longitudinally and parallel. Finally, we observed a specimen where fibers filled the endomysium pockets (Figure 15, panel C).

Acrochordidae Acrochordus granulatus

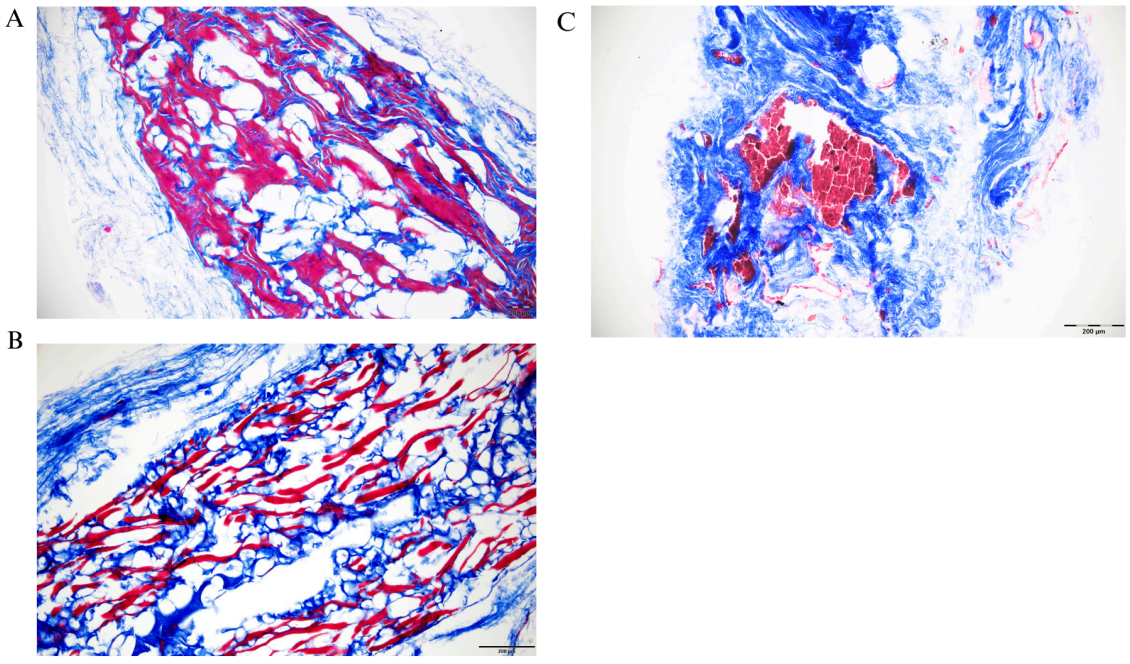

Figure 16: Mason's trichrome of *Acrochordidae Acrochordus granulatus* A) Transverse section at 10x magnification. B) Sagittal section at 10x magnification. C) Muscle fibers at 50x magnification highlighting striated fibers indicative of skeletal muscle

Viperidae Atheris squamigera

Acrochordus granulatus' fiber arrangement was unusual and conclusions are largely speculative. It's difficult to determine the directionality of fibers in a cross section because of the lack of structure of the fascicle (Figure 16 panel A). All specimens of this species had similar results perhaps due to preservation issues. In a longitudinal cross section fibers are more distinctly observed, but there are holes in the epimysium. Finally, we observed a specimen where fibers were more distinct in the transverse, but still are oddly fragmented (Figure 16, panel C).

Viperidae Atheris squamigera

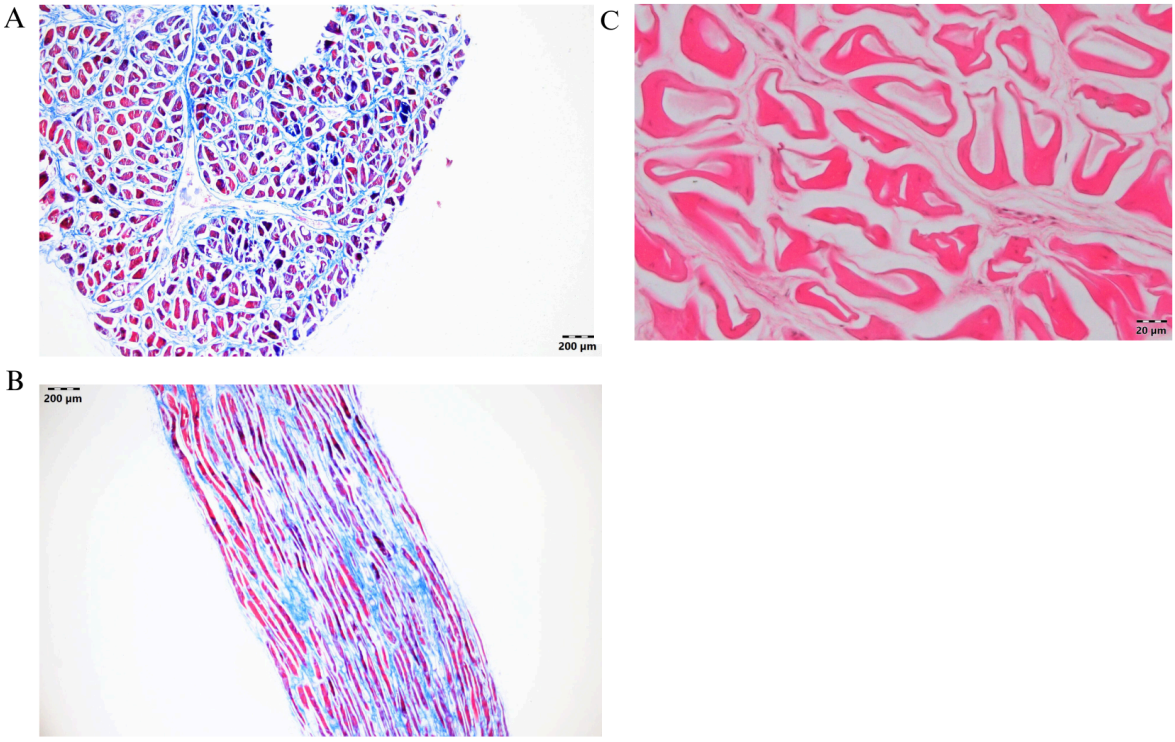

Figure 17: Mason's trichrome of *Viperidae Atheris squamigera* A) Transverse section at 10x magnification. B) Sagittal section at 5x magnification. C) Muscle fibers at 50x magnification highlighting striated fibers indicative of skeletal muscle

In *Atheris squamigera* , the fiber arrangement can offer numerous insights. Fibers are seen to run both longitudinal and pinnate in a cross section (Figure 17 panel A). Similar to Crotalus, most fibers are fairly circular, and their size largely consistent with only shape changing. In this particular specimen, the sinusoid is not completely collapsed, and the perimysium seems thicker surrounding this region with more pinnate (oblong fibers) fibers near the sinusoid. Furthermore, the arrangement seems to have some sort of order with the direction of muscle fibers running largely longitudinal (as seen in panel A). In the longitudinal section (Figure 17, panel B) fibers run longitudinal and parallel. Finally, we observed a specimen where fibers had holes perhaps because of a muscular defect (Figure 17, panel C).

Colubridae Pantherophis alleghaniensis

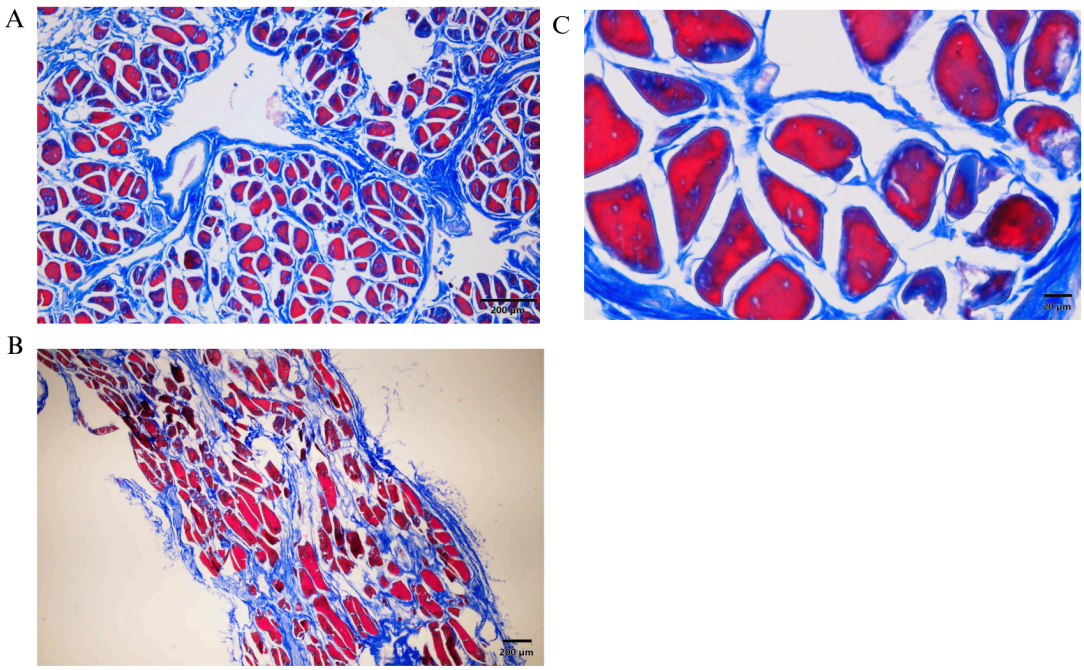

Figure 18: Mason's trichrome of *Colubridae Pantherophis alleghaniensis* A) Transverse section at 10x magnification. B) Sagittal section at 10x magnification. C) Muscle fibers at 50x magnification highlighting striated fibers indicative of skeletal muscle

The fiber arrangement of *Pantherophis alleghaniensis* can offer numerous insights. Fibers are seen to run both longitudinally and pinnately in a cross section (Figure 18 panel A). Similar to Crotalus, most fibers are fairly circular, and their size largely consistent with only shape changing. In this particular specimen, the sinusoid is not completely collapsed and seems to have an interesting wave-like shape; additionally, the perimysium seems thicker surrounding this region with more pinnate (oblong fibers) fibers near the sinusoid. Furthermore, the arrangement seems to have some sort of order (as seen in panel A). In the longitudinal section (Figure 18, panel B) fibers run longitudinal, but whether some run pinnately or if it is simply breakage is unclear. Finally, a closer look of the fibers indicates the difference in shape suggesting directionality of fibers (Figure 18, panel C).

Xenopeltidae Xenopeltis unicolor

A

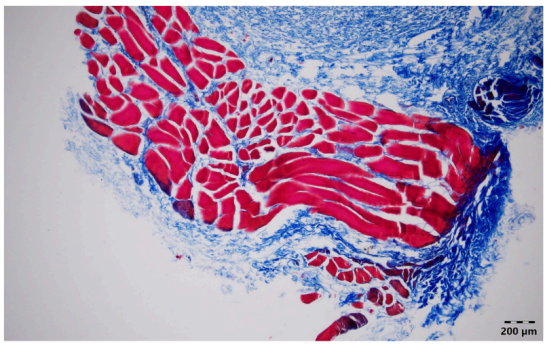

B

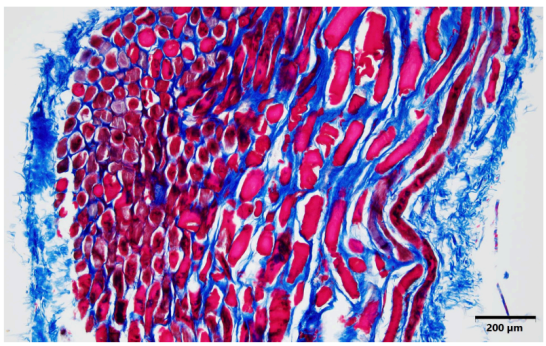

C

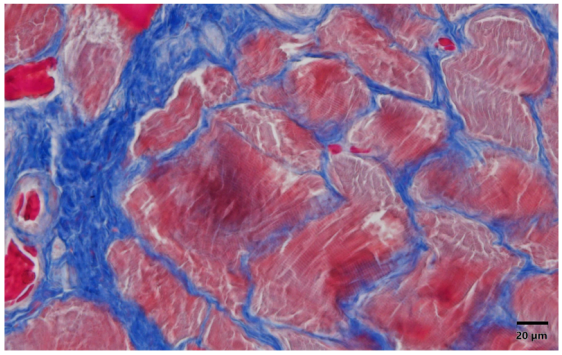

Figure 19: Mason's trichrome of *Xenopeltidae Xenopeltis unicolor* A) Transverse section at 10x magnification. B) Sagittal section at 10x magnification. C) Muscle fibers at 50x magnification highlighting striated fibers indicative of skeletal muscle

Xenopeltis unicolor's fiber arrangement can also provide a plethora of insights. Fibers are seen to run both longitudinal and pinnate in a cross section (Figure 19 panel A). Unlike other species Xenopeltis's fibers vary in size and length in a cross section (Figure 19 panel A). In this particular specimen, the sinusoid is completely collapsed and the perimysium seems thicker and more vast (Figure 19 panel A). Furthermore, the arrangement seems to lack order (as seen in panel A). In the longitudinal section (Figure 19, panel B) fibers run longitudinal and pinnate, but are separated with more longitudinal fibers on one side. Finally, a closer look of the fibers confirms the presence of skeletal muscle (Figure 19, panel C).

Viperidae Crotalus horridus

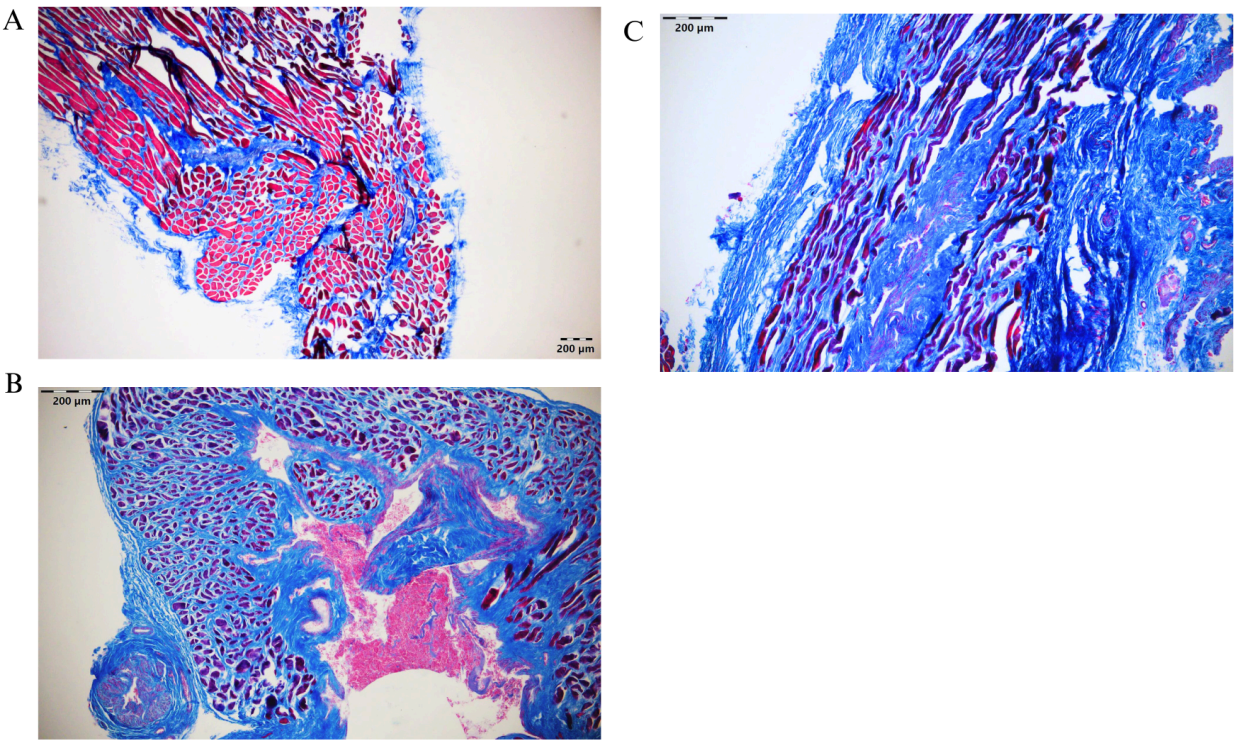

Figure 20: Mason's trichrome of *Viperidae Crotalus horridus* A) Transverse section at 10x magnification. B) Sagittal section at 10x magnification. C) Muscle fibers at 50x magnification highlighting striated fibers indicative of skeletal muscle

We can glean many insights from *Crotalus horridus'* fiber arrangement. Fibers are seen to run both longitudinal and pinnate in a cross section (Figure 20 panel A). Unlike other Crotalus species, fiber arrangement seems random with size and shape differing greatly (Figure 20 panel A). However, in a different specimen fibers are fairly circular, and their size largely consistent with only shape changing (Figure 20 panel B). In this particular specimen, the sinusoid is not completely collapsed, and the perimysium seems thicker surrounding this region; additionally some sort of fluid or tissue was stained (Figure 20 panel B). In the longitudinal section (Figure 20, panel C) fibers run longitudinal and parallel, the perimysium seems extra thick and pockets of fluid or some other substance are observed similar to what is seen in panel B.

Lamprophiidae Mehelya crossi

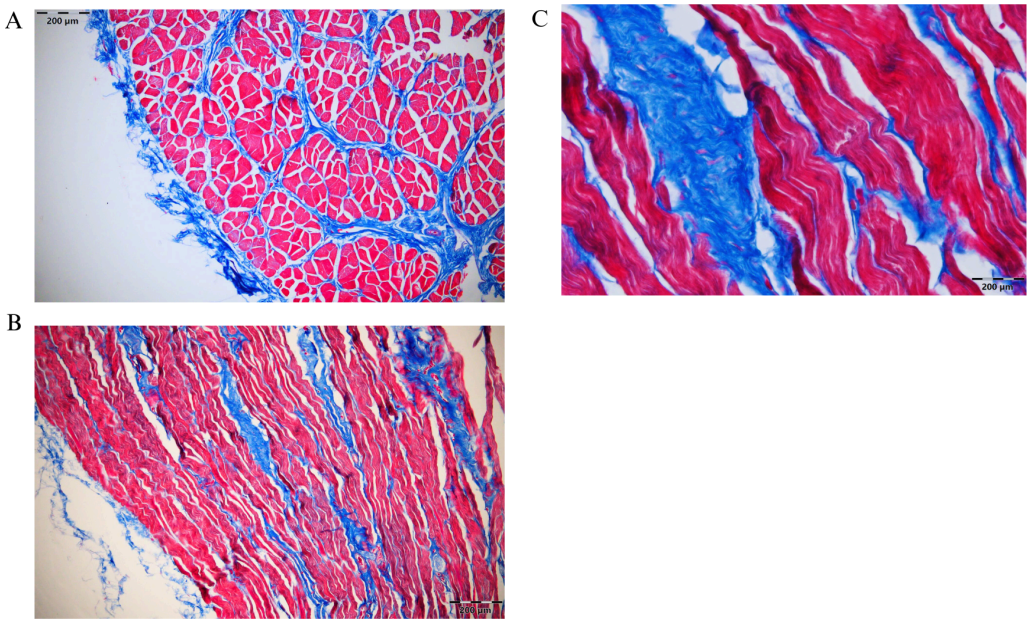

Figure 21: Mason's trichrome of *Lamprophiidae Mehelya crossi* A) Transverse section at 10x magnification. B) Sagittal section at 10x magnification. C) Muscle fibers at 50x magnification highlighting striated fibers indicative of skeletal muscle

In *Mehelya crossi,* we can obtain numerous insights about the fiber arrangement. Fibers are seen to run both longitudinal and pinnate in a cross section, but their shape is less circular and more fibers appear to run pinnately (Figure 21 panel A). In this particular specimen, the sinusoid is completely collapsed and the layers of tissue bundles are more distinctly seen. Furthermore, the arrangement seems to have some sort of order (as seen in panel A). In the longitudinal section (Figure 21, panel B) fibers run longitudinal and parallel. Finally, a closer look of the fibers in longitudinal highlights the wave-like shape of the fibers (Figure 21, panel C).

Boidae Boa constrictor

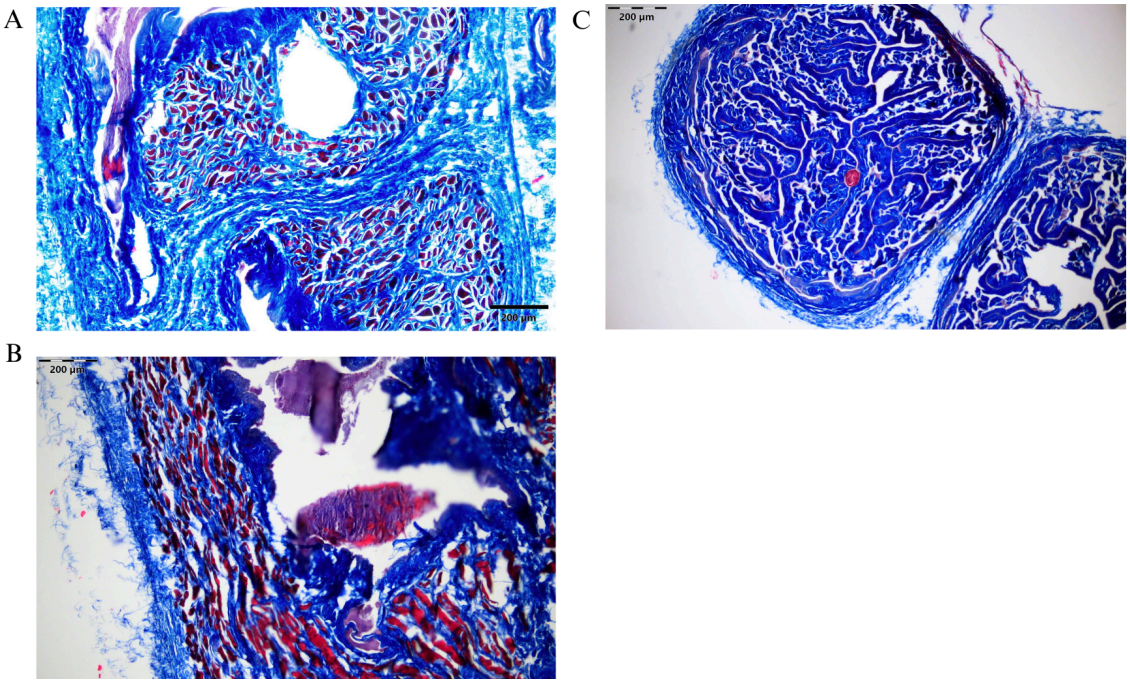

Figure 22: Mason's trichrome of *Boidae Boa constrictor* A) Transverse section at 10x magnification. B) Sagittal section at 10x magnification. C) Muscle fibers at 50x magnification highlighting striated fibers indicative of skeletal muscle

Fiber arrangement in *Boa constrictor* can provide a multitude of interesting insights as well. Fibers are seen to run both longitudinal and pinnate in a cross section, and their shape is largely consistent (Figure 22 panel A). In this particular specimen, the sinusoid is not completely collapsed and the epimysium is thick (as seen in panel A). In the longitudinal section (Figure 22, panel B) fibers run longitudinal and parallel, but some fibers appear to run pinnately as well. Finally, unlike other specimens, a sample was taken at the anterior end of the RPM, fibers are largely absent and the collapsed sinusoid provides insight into how this muscle opens at the attachment point of the hemipene (Figure 22, panel C).

Pythonidae Python bivittatus

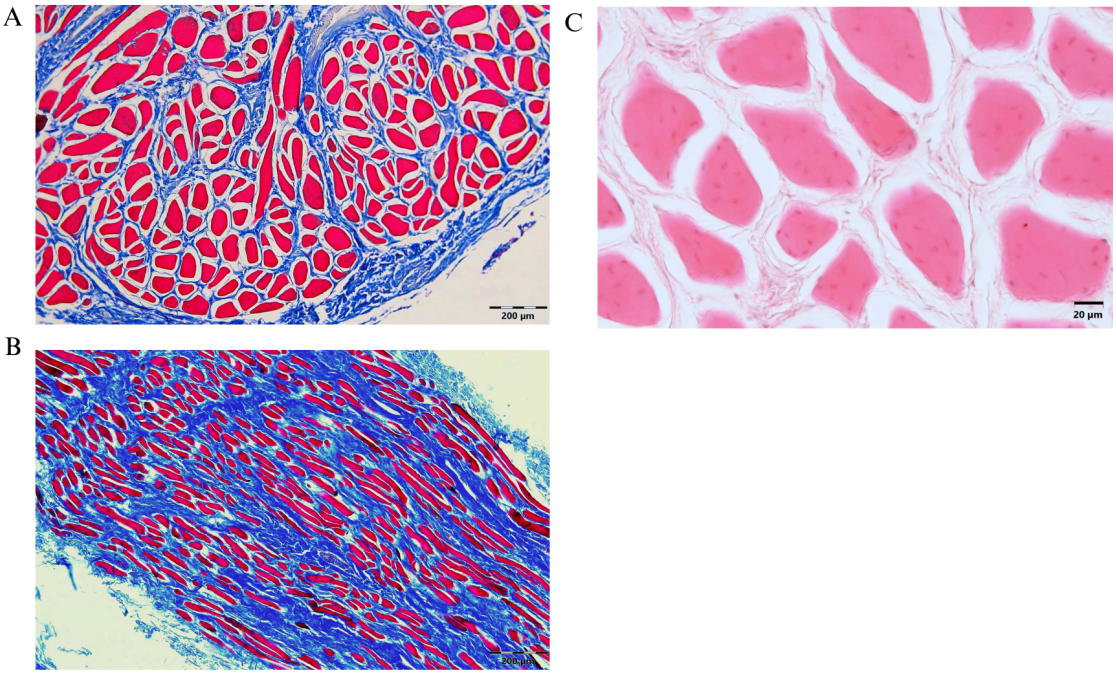

Figure 23: Mason's trichrome of *Pythonidae Python bivittatus* A) Transverse section at 10x magnification. B) Sagittal section at 10x magnification. C) Muscle fibers at 50x magnification highlighting striated fibers indicative of skeletal muscle

Lastly, the fiber arrangement in *Python bivittatus* can provide valuable insights as well. Fibers are seen to run both longitudinal and pinnate in a cross section, notably larger more pennate fibers seem to run closer to the middle (Figure 23 panel A). In the longitudinal section (Figure 23, panel B) fibers run longitudinal and parallel, but some fibers appear to run pinnately as well. Finally, a close examination of the fibers from an H&E stain reveals the multitude of nuclei in the muscle cells and the differences in shape (Figure 23, panel C).

Statistical Analysis of Fiber Arrangement

Fiber arrangement was assessed utilizing ImageJ's automatic particle output for each specimen. Specifically focusing on the fiber diameter (denoted as Feret), density of fibers (% area of fibers in image), RPM diameter (obtained from sagittal images) and fiber count (from transverse). I then ran general linear model analysis on the species I had the most specimens for which were *Crotalus scutulatus* and *Python bivittatus:*

Crotalus Scutulatus Fiber Measurements

In order to assess whether a larger fiber diameter was associated with a

larger hemipene volume, I conducted a linear regression The volume of the hemipenes is not significantly associated with fiber diameter in *Crotalus scutulatus*, $F(1, 6) = 0.6659$, $MSE = 404.91$, $p < 0.4457$ (Figure 24).

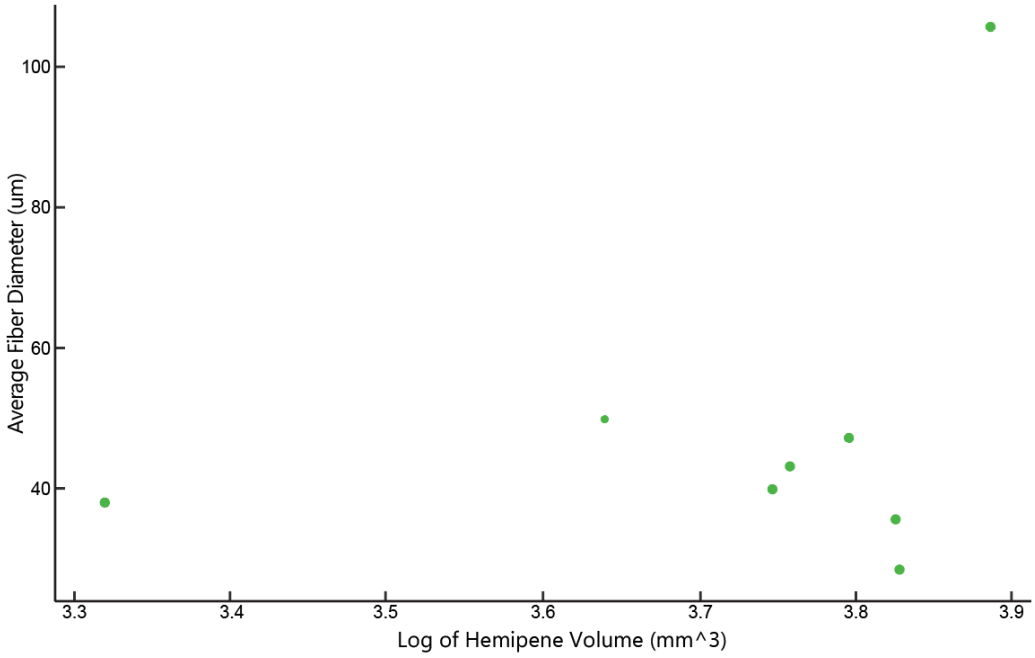

Figure 24: General linear regression model depicting average fiber diameter by the log value of hemipene volume for *Crotalus scutulatus.*

Similarly, I conducted a linear regression to determine whether RPM diameter was a predictor of hemipene volume, such that a larger muscle diameter

would indicate a larger hemipene. The volume of the hemipene is significantly associated with muscle diameter in *Crotalus scutulatus*, F(1, 6) = 6.2983, MSE = 4.1291, p < 0.04593 (Figure 25).

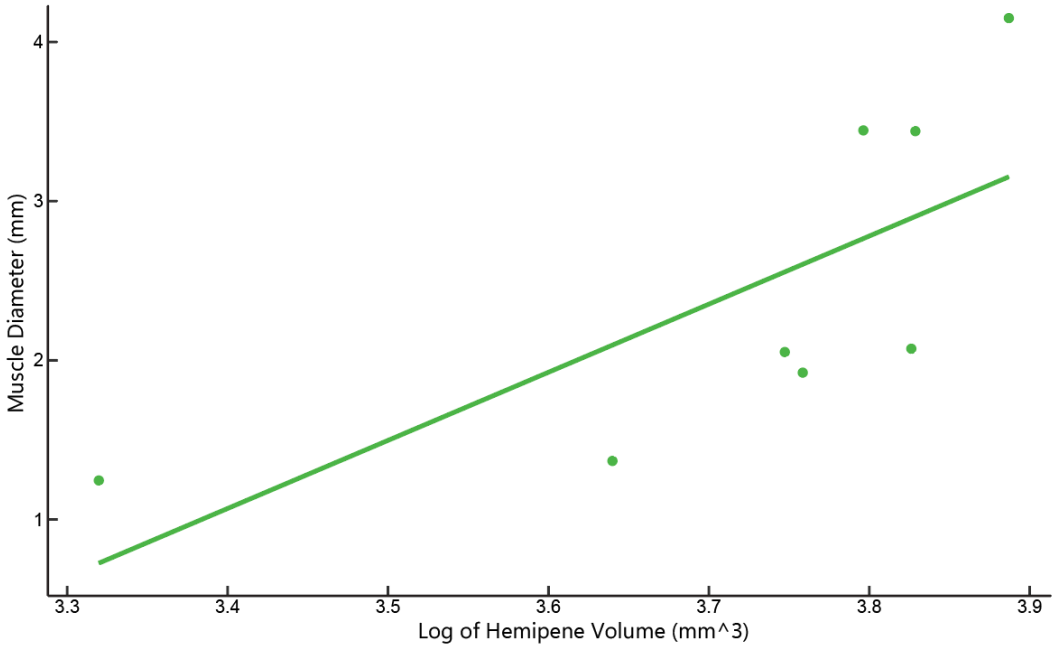

Figure 25: General linear regression model depicting muscle diameter in mm by the log value of hemipene volume for *Crotalus scutulatus.*

I conducted a linear regression to determine whether density of fibers was a predictor of hemipene volume. Such that a higher density of fibers would indicate a larger hemipene. The volume of the hemipenes is not significantly associated with muscle diameter in *crotalus scutulatus*, F(1, 6) = 0.3636, MSE =

19.542, p < 0.5686 (Figure 26).

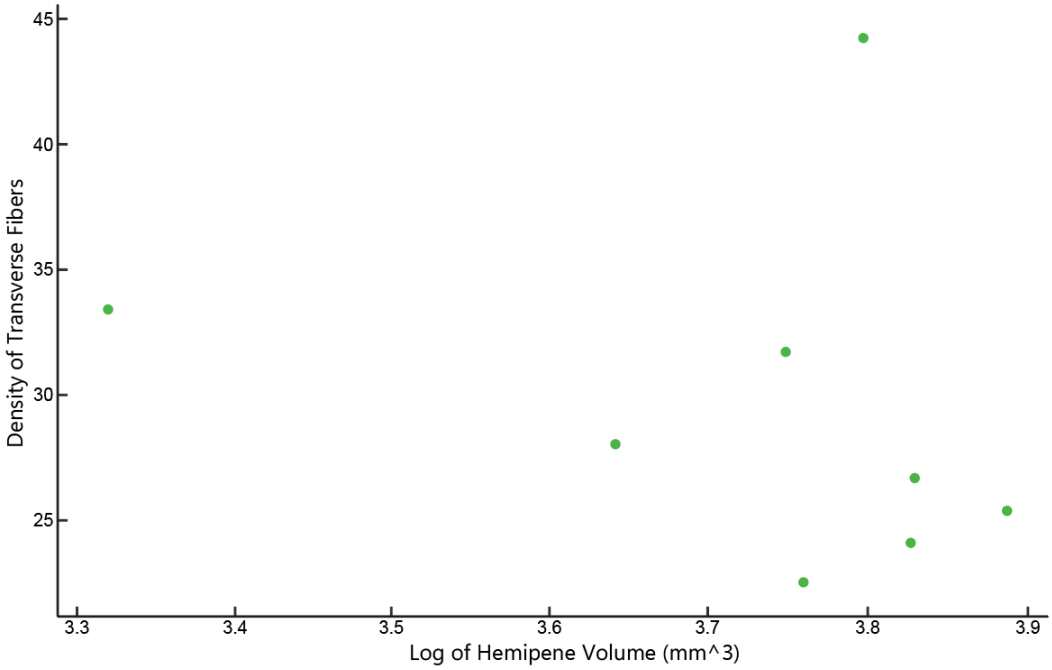

Figure 26: General linear regression model depicting density of fibers by the log value of hemipene volume for *Crotalus scutulatus.*

Lastly, I conducted an ANOVA to determine whether total count of fibers was a predictor of hemipene volume. Such that more fibers in the transverse would indicate a larger hemipene. The volume of the hemipenes is not significantly associated with fiber count in *Crotalus scutulatus*, F(1, 6) = 1.9984, MSE = 35690, p < 0.2072 (Figure 27).

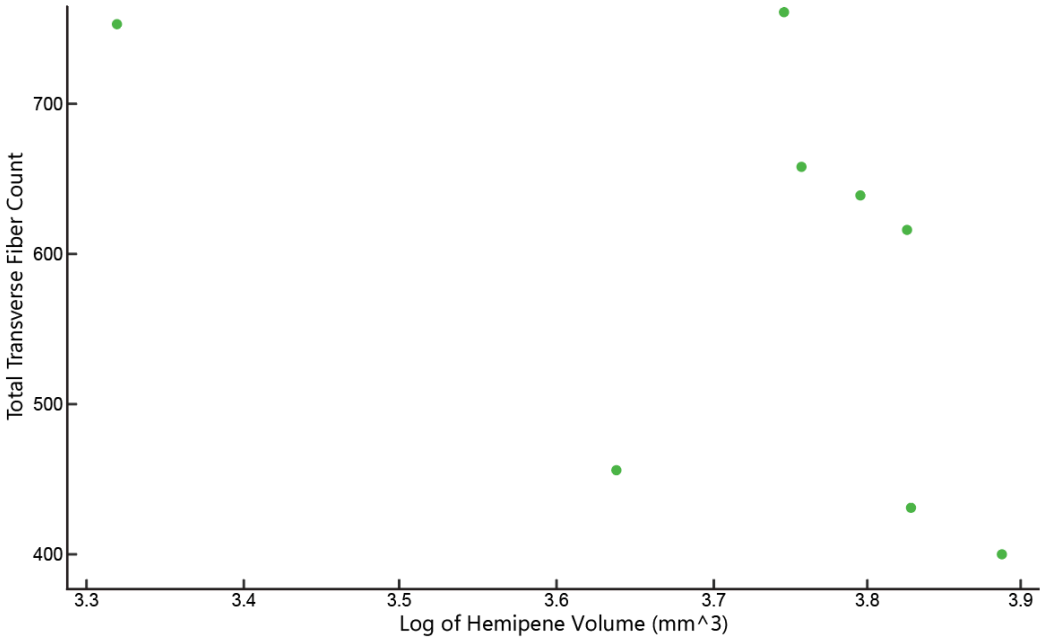

Figure 27: General linear regression model depicting fiber count by the log value of hemipene volume for *Crotalus scutulatus.*

Python Bivittatus Fiber Measurements

In order to assess whether a larger fiber diameter was predicted by a larger hemipene volume, I conducted a one-way analysis of variance (ANOVA). The volume of the hemipenes is not significantly associated with fiber diameter in *python bivittatus*, $F(1, 5) = 1.7902$, MSE =384.29, $p < 0.2733$ (Figure 28).

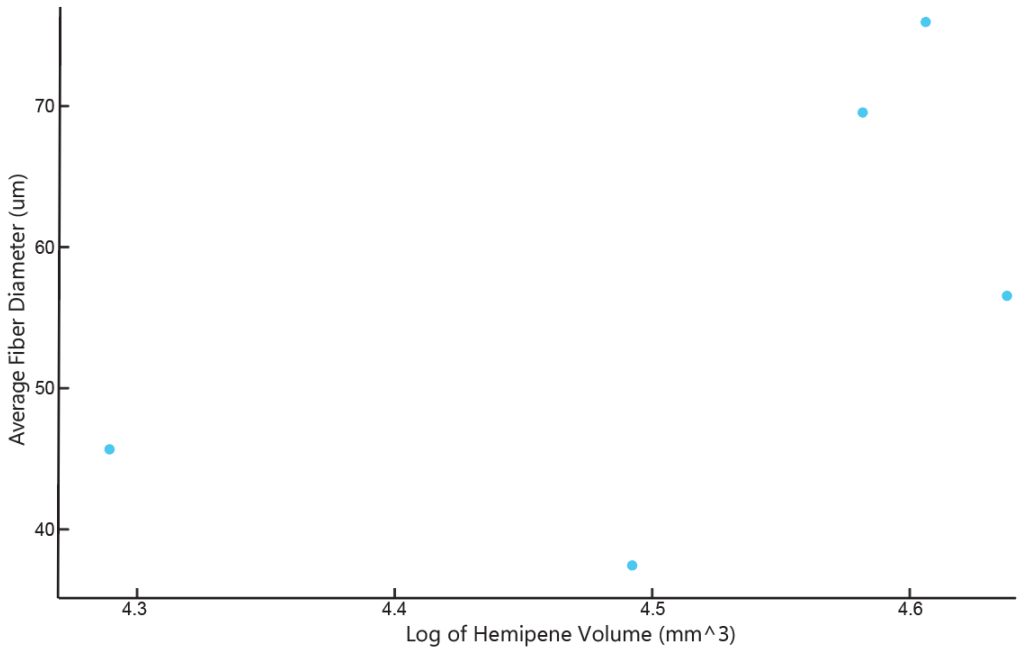

Figure 28: General linear regression model depicting average fiber diameter by the log value of hemipene volume for *Python bivittatus*.

Similarly, I conducted an ANOVA to determine whether RPM diameter was a predictor of hemipene volume, such that a larger muscle diameter would indicate a larger hemipene. The volume of the hemipenes is not significantly associated with muscle diameter in *python bivittatus* $F(1, 5) = 1.1793$, MSE = 0.54344, $p < 0.3569$ (Figure 29).

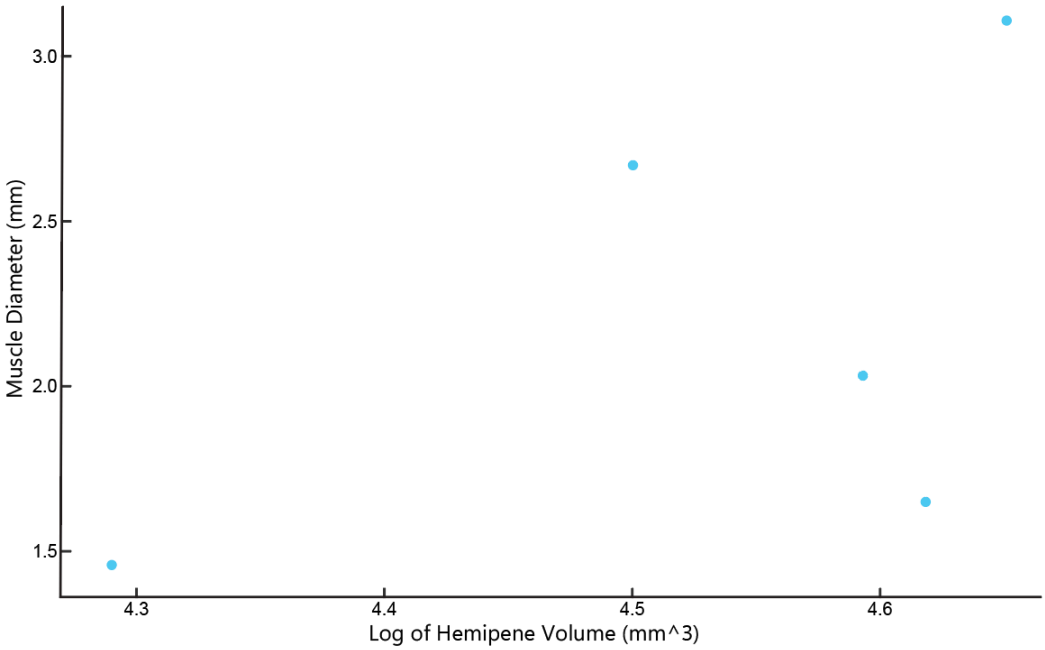

Figure 29: General linear regression model depicting muscle diameter in mm by the log value of hemipene volume for *Python bivittatus*.

I conducted an ANOVA to determine whether density of fibers was a predictor of hemipene volume, such that a higher density of fibers would indicate a larger hemipene. The volume of the hemipenes is not significantly associated with muscle diameter in *Python bivittatus*, $F(1, 5) = 0.0479$, $MSE = 2.038$, $p < 0.8408$ (Figure 30).

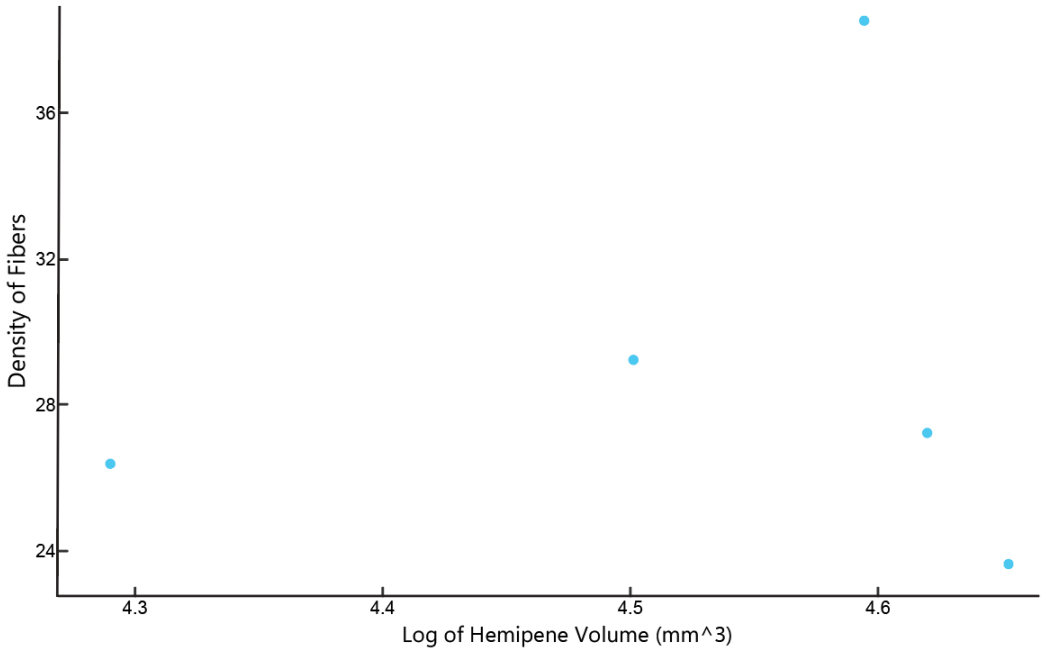

Figure 30: General linear regression model depicting density of fibers by the log value of hemipene volume for *Python bivittatus.*

Finally, I conducted an ANOVA to determine whether total count of fibers was a predictor of hemipene volume, such that more fibers in the transverse would indicate a larger hemipene. The volume of the hemipenes is not significantly associated with fiber count in *python bivittatus*, $F(1, 5) = 0.2185$, $MSE = 22899$, $p < 0.6721$ (Figure 31).

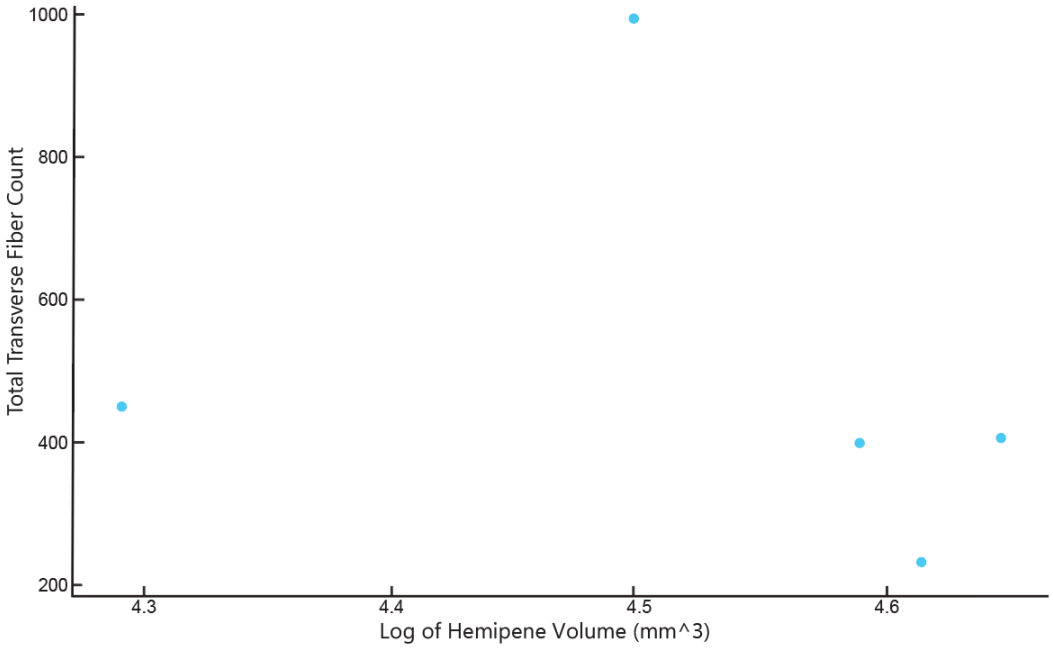

Figure 31: General linear regression model depicting fiber count by the log value of hemipene volume for *python bivittatus*.

I also ran a linear model with the combined data from all 12 species to determine the overall relationship between total density, fiber diameter, total muscle diameter compared to hemipene volume. The ANOVA results showed that the combined effect of muscle diameter and percent area was significantly associated with hemipene volume ($F(1, 33) = 12.2102$, $MSE = 3.04259$, $p < 0.001377$). Individually the variables did not have a significant effect on hemipene length.

Discussion

The results obtained from this research shed light on the specific adaptations of the *retractor penis magnus* across snake species, facilitating a deeper understanding of their reproductive strategies. Through tissue quantification, macrodissection, and histological observations this study aimed to understand the RPM's function, compare various snake species, and explore potential variations in the muscle's structure across these species. This combined approach of qualitative and quantitative analysis allowed us to target the questions surrounding the purpose and functioning of this structure more effectively.

Through statistical analysis, this study aimed to target the question of does size matter. This question was inspired by an observation made in the Brennan lab that the size of the RPM does not seem to correlate with the size of the hemipenis. If this is the case, what aspect of the snake is controlling for the length of the RPM? Through initial analysis across three species we found that RPM length is significantly related to body size (SVL) and hemipene volume, but not tail length. Additionally, we found that the combined effect, as well as the individual effect of these variables, was statistically significant for hemipene volume and SVL. Thus despite initial observations, the size of the hemipene does appear to have an effect on the length of the RPM. For Bivittatus and Rhombifer this relationship was positive such that a larger hemipene was associated with a longer RPM. However,

we observed the inverse relationship for Scutulatus. This difference could be because Scutulatus have rattles and thus have constraints in the length of their RPM. Thinking back to our understanding of force and length of the RPM, a longer RPM would have a faster retraction than a shorter RPM which would be beneficial for a large hemipenis. Scutulatus hemipenes have more spines than Rhombifer and Bivittatus, so having a shorter RPM that could allow for a slower contraction, and thus decrease the likelihood of accidental injury from the spines would be beneficial. We expected there to be some sort of relationship between tail length and RPM length given that a larger snake (SVL) tended to have a longer RPM; however, this was not the case. This suggests that either a longer RPM that can exert greater force in retraction is necessary or perhaps that an RPM with a greater diameter is necessary with tail constraints like those in Scutulatus. However with the current sample size it's hard to answer this definitively, but it appears that there is some sort of general relationship between both of these structures and that this varies vastly between species.

Through histological analysis and macrodissection, this study delved deeper into the morphology of this structure to gain a more comprehensive understanding of its function. We observed how the fibers in this muscle and how the muscle itself, as seen during macrodissections, is able to stretch around the sinusoid. Thinking back to the findings in Porto et al. (2013), these spaces are

most likely for blood vessels, suggesting that this muscle may play a role in providing rigidity for the hemipenis during copulation. If this secondary function is correct, we would expect that the arrangement of the muscle fibers may play an important role in pushing blood from the muscle into the hemipene during copulation. Across all 12 species, we observed how fibers ran both pinnately and longitudinally supporting this hydrostatic property hypothesis (Kier and Smith, 1985). In particular, across several species the fibers surrounding the sinusoid appeared to be more pinnate suggesting that shortening of these fibers and lengthening of longitudinal fibers could allow for blood to flow quickly through this space and into the hemipenis attachment. Additionally, we observed how several species had breakage of fibers indicating the recent use of these muscles. Thinking back to the findings of Martin et al. (2021), they found a relationship between muscle use and inflammation, but not between the body size and hemipene size, which is an interesting difference that requires more attention.

Beyond visual differences, I analyzed the statistical differences in fiber composition across species. Larger fibers, a larger muscle, and a more dense fascicle would contribute to greater force production. I expected that if this muscle was responsible for both pulling in the hemipene quickly and providing rigidity by playing a role in eversion of the hemipene that the fibers would have statistical significance for that. However, my results were largely insignificant.

This is most likely a result of the small sample size I had within species. I did find a significant result for the relationship between muscle diameter and hemipene volume in *Crotalus scutulatus*. Thinking back to the results for tail length being largely insignificant it makes sense that these muscles thickness would play a larger role in this species. Comparing across all species, I found that the combined effect of muscle diameter and percentage of area fibers occupied (more dense fibers) had a significant relationship with hemipene volume. This makes sense when we think of force muscle can produce and that a larger more densely packed muscle could exert more force.

However there have been several limitations to this study. Primarily the learning curve of histology as it takes a while to master the skill set required to obtain meaningful results. Another major limitation to this study was the sample size for each species. Despite having a large sample size of snakes, RPM's were not always taken. For instance, we had many Nerodia species, but only *Nerodia rhombifer* had RPM's taken. Additionally, the Colubridae family has a tendency to have tail breakage and thus many of the tail length measurements were not recorded during dissection (Mendelson, 1992). So for comparison in this thesis, many species were not included because either the tail measurement was not obtained or because the RPM length was not taken initially when the sample was collected.

Regardless of these limitations, the insights gained from this research have the potential to extend beyond the understanding of snake reproductive organs. They could have broader implications for areas such as sexual selection, reproductive strategies, and evolutionary patterns in snakes, and possibly even in other reptiles. By shedding light on the complex interplay between form and function in snake reproductive organs, this study seeks to contribute valuable insights into the evolutionary biology of snakes.

In conclusion, this comparative analysis of the morphological characteristics of the retractor penis muscle in snakes aims to enhance our understanding of this structure's role and functioning. The combination of these statistical analyses provided a robust and comprehensive approach for analyzing the relationship between hemipene size and retractor penis muscle length, allowing for accurate and reliable statistical inference. By employing histological analysis and comparing the muscle across different snake families, the study expects to provide valuable insights into the evolutionary biology of snakes and potentially other reptiles. This research has the potential to contribute significantly to our knowledge of snake evolutionary biology and offer valuable insights into the broader field of reproductive biology

APPENDIX

Table 1. Protocol used for processing formalin-preserved specimens.

Procedure	Chemicals	Time	Temperature (°C)
Dehydration I	70% EtOH	1 hr	Room temperature
Dehydration II	95% EtOH	1 hr	Room temperature
Dehydration III	100% EtOH I	1 hr	Room temperature
Dehydration IV	100% EtOH II	1 hr	Room temperature
Dehydration V	100% EtOH III	4 hr/overnight	Room temperature
Clearing I	1:1 Histoclear+EtOH	30 min	Room temperature
Clearing II	100% Histoclear I	30 min	Room temperature
Clearing III	100% Histoclear II	30 min	Room temperature
Clearing IV	1:1 Histoclear+Paraffin	15 min	54
Infiltration I	Paraffin I	30 min	54
Infiltration II	Paraffin II	30 min	54
Infiltration III	Paraffin III	1 hr	54

Table 2. Protocol used for Masson's Trichrome staining.

Chemicals	Time
Histoclear I	5 min
Histoclear II	2 min
100% EtOH	2 min
95% EtOH	2 min
70% EtOH	4 min
50% EtOH	2 min
35% EtOH	2 min
dH2O	2 min
Bouin's solution	1 hr (at 54°C)
Masson A	1.5 min
Masson B	1.5 min
Masson C	25 s
1% Acetic Acid	2.5 min
1:1 Acetic Acid+EtOH	30 s
100% EtOH rinse	(twice)
Histoclear rinse	(twice)

Table 3. Protocol used for H&E staining.

Chemicals	**Time**
Histoclear (I)	5 min
Histoclear (II)	2 min
100% EtOH	2 min
95% EtOH	2 min
70% EtOH	2 min
50% EtOH	2 min
35% EtOH	2 min
Water	2 min
Hematoxylin	20s
35% EtOH	2 min
50% EtOH	2 min
95% EtOH	2 min
Eosin Y	2 min
95% EtOH	2 min
100% EtOH (I)	2 min
100% EtOH (II)	2 min
Histoclear (I)	5 min
Histoclear (II)	5 min

Figure 32. Illustration of skeletal muscle fiber and corresponding structures in Mason's trichrome slide.

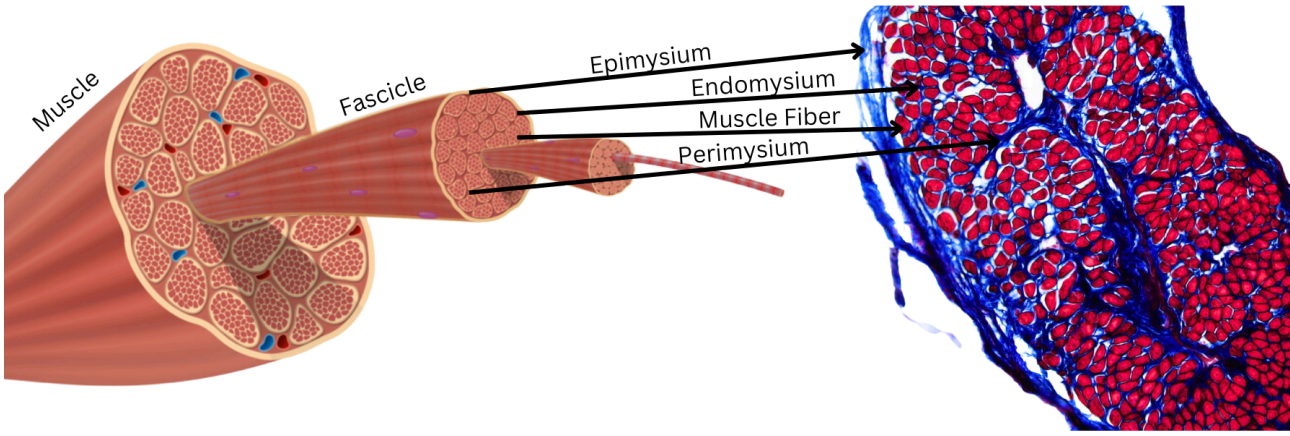

RCode:

```
############################
#      Autumn Lee      #
#  GLM Workflow for RPM #
############################
setwd("C:/Users/Autumn/OneDrive/Desktop/WD")
RPM_SVL<-read.csv("SVL.csv")
view(RPM_SVL)
RPM_Tail<-read.csv("Tail_Length.csv")
view(RPM_Tail)
RPM_Hemi<-read.csv("Hemipene.csv")
view(RPM_Hemi)
```

```
RPM_comparison<-read.csv("RPM_comparison.csv")
view(RPM_comparison)

#### RPM length x hemi V
ggplot(data=RPM_Hemi, aes(x=Log_10_HP_vol, y=RPM_L, color=Species))+
  geom_point()+
  geom_smooth(method='lm', se=FALSE)
lm1<-lm(RPM_L ~ Log_10_HP_vol * Species_code, data=RPM_Hemi)
summary(lm1)
anova(lm1)

#### RPM length x SVL
ggplot(data=RPM_SVL, aes(x=SVL_Log, y=RPM_L,color=Species))+
  geom_point()+
  geom_smooth(method='lm', se=FALSE)

lm2<- lm(RPM_L ~  SVL_Log, data=RPM_SVL)
summary(lm2)
anova(lm2)
```

```
#### RPM length x tail length


ggplot(data=RPM_Tail, aes(x=Tail.Log_mm, y=RPM_L,color=Species))+
  geom_point()+
  geom_smooth(method='lm', se=FALSE)
lm3<-lm(RPM_L ~ Tail.Length_mm * Species, data=RPM_Tail)
summary(lm3)
anova(lm3)


###RK - might be good to also report just raw RPM to tail relationship?
lmtest2<-lm(RPM_L ~ Tail.Length_mm, data=RPM_Tail)
summary(lmtest2)
anova(lmtest2)


##### All variables x RPM length
Model<-lm(RPM_L ~ Log_10_HP_vol + SVL_Log * Log_10_HP_vol,
data=RPM_comparison)
summary(Model)
anova(Model)
```

```
############################
#      Autumn Lee          #
# GLM Workflow for Fibers #
############################
# Using tidyverse
library(ggplot2)
library(tidyverse)
# Renamed data set
setwd("C:/Users/Autumn/OneDrive/Desktop/WD")
CRSC_Fiber<-read.csv("CRSC_Fiber.csv")
view(CRSC_Fiber)
PYBI_Fiber<-read.csv("PYBI_Fiber.csv")
view(PYBI_Fiber)
Fiber_ALL<-read.csv("Fiber_ALL.csv")
view(Fiber_ALL)

##HV x fiber diameter

ggplot(data=CRSC_Fiber, aes(x=Log_10_HP_vol, y=Feret_Diameter))+
```

```
  geom_point()+
  geom_smooth(method='lm', se=FALSE)

ggplot(data=CRSC_Fiber, aes(x=Hemipene_Volume_mm.3, y=Feret_Diameter))+
  geom_point()+
  geom_smooth(method='lm', se=FALSE)

ggplot(data=PYBI_Fiber, aes(x=Log_10_HP_vol, y=Feret_Diameter))+
  geom_point()+
  geom_smooth(method='lm', se=FALSE)

ggplot(data=Fiber_ALL, aes(x=Log_10_HP_vol, y=Feret_Diameter,
color=Species))+
  geom_point()+
  geom_smooth(method='lm', se=FALSE)

##HV x muscle diameter

ggplot(data=CRSC_Fiber, aes(x=Log_10_HP_vol, y=muscle_diameter))+
  geom_point()+
```

```
  geom_smooth(method='lm', se=FALSE)

ggplot(data=PYBI_Fiber, aes(x=Log_10_HP_vol, y=muscle_diameter))+
  geom_point()+
  geom_smooth(method='lm', se=FALSE)

ggplot(data=Fiber_ALL, aes(x=Log_10_HP_vol, y=muscle_diameter,
color=Species))+
  geom_point()+
  geom_smooth(method='lm', se=FALSE)


##HV x percent area

ggplot(data=CRSC_Fiber, aes(x=Log_10_HP_vol, y=perc_Area_Transverse))+
  geom_point()+
  geom_smooth(method='lm', se=FALSE)

lm1<-lm(perc_Area_Transverse ~ Log_10_HP_vol, data=CRSC_Fiber)
summary(lm1)
```

```
anova(lm1)

ggplot(data=PYBI_Fiber, aes(x=Log_10_HP_vol, y=perc_Area_Transverse))+
  geom_point()+
  geom_smooth(method='lm', se=FALSE)

ggplot(data=Fiber_ALL, aes(x=Log_10_HP_vol, y=perc_Area_Transverse,
color=Species))+
  geom_point()+
  geom_smooth(method='lm', se=FALSE)


## LM total density, fiber diameter, total muscle diameter, measure for hemi
volume
Fibercompare<-lm(Log_10_HP_vol ~ Feret_Diameter  + muscle_diameter *
perc_Area_Transverse , data=Fiber_ALL)
summary(Fibercompare)
anova(Fibercompare)
```

LITERATURE CITED

Bassett, E., G. (1961). Observations on the retractor clitoridis and retractor penis muscles of mammals, with special reference to the ewe. *Journal of Anatomy* 95(1), 61-77.

Bento, H., J., Ferreira, A., & da Paz, R., C., R. (2022). Brazilian Boidae hemipenis morphology: Macroscopic and histological aspects. *Anatomia, Histologia, Embryologia*, 51, 781–785. https://doi.org/10.1111/ahe.12856

Clark, H. (1945). The Anatomy and Embryology of the Hemipenis of Lampropeltis, Diadophis and Thamnophis and Their Value as Criteria of Relationship in the Family Colubridae, Proceedings of the Iowa Academy of Science, 51(1), 411-445.

Dowling, H., G, & Savage, J., M. (1960). A Guide to the Snake Hemipenis: A Survey of Basic Structure and Systematic Characteristics, *Zoologica*, biostor.org/reference/194094.

Edward, T. (1960).Vipera Caudi-Sona Americana, Or the Anatomy of a Rattle-Snake, Dissected at the Repository of the Royal Society, *Philosophical Transactions*, 13, 25–46.

Folwell, M., J., Sanders K., L., Brennan P., L., R., & Crowe-Riddell J., M. (2022). First evidence of hemiclitores in snakes, Proc. R. Soc. http://doi.org/10.1098/rspb.2022.1702

Gredler, M., L., Sanger, T., J., & Cohn, M., J. (2014). Development of the Cloaca, Hemipenes, and Hemiclitores in the Green Anole, Anolis carolinensis. *Sexual Development*, 9, 21 - 33.

Jensen, G. W., et al. (2022). Chronic multi-electrode electromyography in snakes. *Frontiers in Behavioral Neuroscience*, vol. 15 https://doi.org/10.3389/fnbeh.2021.761891.

Kelly, D A. Penile anatomy and hypotheses of erectile function in the American Alligator (alligator mississippiensis): Muscular eversion and elastic retraction. *The Anatomical Record*, 296(3), 488–494, https://doi.org/10.1002/ar.22644

Kelly, D. A. (2002). The Functional Morphology of Penile Erection: Tissue Designs for Increasing and Maintaining Stiffness, Integrative and *Comparative Biology*, 42(2), 216–221, https://doi.org/10.1093/icb/42.2.216.

Keough, J., S. Evolutionary implications of hemipenial morphology in the terrestrial Australian Elapid Snakes, *Zoological Journal of the Linnean Society*, 125(2), 239–278, https://doi.org/10.1111/j.1096-3642.1999.tb00592.x.

Kier, W., M., Smith, K., K. (1985). Tongues, tentacles and trunks: the

biomechanics of movement in muscular-hydrostats. *Zoological Journal of the Linnean Society*, 83: 307-324. https://doi.org/10.1111/j.1096-3642.1985.tb01178.x

King, A., S. (1981). Phallus. In: King AS, McLelland J, editors. Form and function in birds, *Academic Press,* 2, 107–147.

Martin, K. S., et al. (2021). Use it and bruise it: Copulation rates are associated with muscle inflammation across anole lizard species. *Journal of Zoology*, 314, (3), 187–193, https://doi.org/10.1111/jzo.12880.

Mendelson, J., R. (1992). Frequency of Tail Breakage in Coniophanes Fissidens (Serpentes: Colubridae). *Herpetologica*, 48(4), 448–55 http://www.jstor.org/stable/3892865.

Murphy, J., B., & Barker D., G. (1980). Courtship and copulation of the Ottoman viper (Vipera xanthina) with special reference to the use of the hemipenes. *Herpetologica*, 36: 165–170.

Olsson, M., & Madsen, T. (1998). Sexual selection and sperm competition in reptiles. In: Birkhead TR, Moller AP eds. Sperm competition and sexual selection. San Diego, CA: *Academic Press*, 503–577.

Porto, Marcovan, et al. (2013). The evolutionary implications of hemipenial morphology of Rattlesnake Crotalus durissus terrificus (Laurent, 1768) (Serpentes: Viperidae: Crotalinae), *PLoS ONE*, 8(6), https://doi.org/10.1371/journal.pone.0066903.

Pisani, G., R. (1976). Comments on the courtship and mating mechanics of Thamnophis (Reptilia, Serpentes, Colubridae), *Journal of Herpetology* 10: 139–142.

Reese, A., M. (1947). The Hemipenes of Copperhead Embryos. *Herpetologica*, *3*(6), 206–208. http://www.jstor.org/stable/3889582